

FT-NIR CONTINUOUS MONITORING OF THE REAGENT  
PREPARATION OF AMINE ALONG WITH THE BATCH-TO-  
CONTINUOUS CONVERSION OF THE PROCESS.

by

Mohammad Hussein

Submitted in partial fulfilment of the requirements  
for the degree of Master of Applied Science

at

Dalhousie University

Halifax, Nova Scotia

February, 2017

© Copyright by Mohammad Hussein, 2017

# Table of Contents

List of Figures.....	iv
List of Tables .....	vii
Abstract.....	viii
List of Abbreviations Used.....	ix
Chapter 1 Introduction.....	1
Chapter 2 Review of Spectrophotometric Methods.....	5
Chapter 3 Mixing Studies.....	9
3.1 Introduction.....	9
3.2 Experimental Setup .....	11
3.3 Results & Discussion.....	14
3.4 Conclusion .....	24
Chapter 4 Liquid Amine Monitoring in Oil .....	25
4.1 Introduction.....	25
4.2 Experimental Procedure .....	27
4.3 Results & Discussion.....	29
4.4 Conclusion .....	33
Chapter 5 Solid NaSt. weight percent monitoring .....	34
5.1 Introduction.....	34
5.2 Experimental Setup .....	35
5.3 Results & Discussion.....	37
5.4 Conclusion .....	42
Chapter 6 Mini-fluidic Continuous Amine Monitoring .....	44
6.1 Introduction.....	44
6.2 Experimental Setup .....	45
6.2.1 Lab Setup.....	45
6.2.2 Spectrophotometry .....	47
6.3 Results and Discussion.....	47

<i>6.3.1 Slope models</i> .....	48
<i>6.3.2 Single-point ratio models</i> .....	51
<i>6.3.3 Two-Point normalization model</i> .....	55
<i>6.3.4 Antaris II TQ-Analyst Results</i> .....	58
<b>6.4 Conclusion</b> .....	61
<b>Chapter 7 Conclusion</b> .....	63
<b>References</b> .....	65
<b>Appendix A</b> .....	69

## List of Figures

Figure 1-1: main unit operations of the potash extraction process. ....	1
Figure 3-1 Schematic of the batch reagent preparation and the continuous inline preparation. ....	12
Figure 3-2: Schematic of the constructed flow loop with the vertical visualization region depicted (inset) for an empty 2” pipe downstream of the injection point. ....	13
Figure 3-3: Illustration of post-processing method applied to videos captured for each mixing configuration. Raw (a), background corrected at pre-injection (b) and injection conditions (c), and normalized variation during injection (d).....	14
Figure 3-4: Amine injection into a 2” Koflo mixer: raw images (top), background corrected (middle) and variance normalized (bottom). Background corrected images appear white as amine is injected, while variance normalized images appear white as the column appearance approaches that of well-dispersed conditions. ....	15
Figure 3-5: Normalized average intensity vs position (mixing element) within the 2” Koflo mixer during injection. Note that at t~18 seconds full recirculation occurs and all intensities approach 1. ....	17
Figure 3-6: Amine injection into a 2” pipe with no mixing element or orifice: raw images (left) and variance normalized (right). Flow is in the upward direction. ....	18
Figure 3-7: Amine injection into a 2” pipe with an orifice ( $\beta=0.7$ ): raw images (left) and variance normalized (right). Flow is in the upward direction. ....	20
Figure 3-8: Normalized average intensity vs time for the 2” configurations. Note that amine injection was stopped at 10s and 12s for the orifice test and “alone” test, respectively. Continuous amine injection was performed for the system using the Koflo mixer. ....	21
Figure 3-9: Variance normalized images during amine injection into a 1” pipe without (left) and with (right) and orifice plate present ( $\beta=0.7$ ). Flow is in the upward direction. ....	23
Figure 3-10: Normalized average intensity vs time for the 1” pipe configurations with and without an orifice present. ....	24
Figure 4-1: ThermoScientific FT-NIR.....	26
Figure 4-2 : The entire spectra of the solution for various amine wt% concentrations .....	26
Figure 4-3: Top to bottom: 2 <sup>nd</sup> derivative, 1 <sup>st</sup> derivative, and raw spectra of the second overtone. ....	28
Figure 4-4: First derivative of the third overtone.....	29
Figure 4-5: Calibration plot for R-NH <sub>2</sub> with temperature effect included.....	30

Figure 4-6: Residual error plot of actual vs. predicted for the 1 <sup>st</sup> derivative analysis of the 2 <sup>nd</sup> and 3 <sup>rd</sup> overtones.....	30
Figure 4-7: PRESS plot for Armeen T in light oil. ....	31
Figure 4-8: Residual error plot for 1st derivative spectra of both the 2nd overtone and 3rd overtone without the temperature correction included. ....	31
Figure 4-9: Residual error plots of 1st derivative with T correction, 2nd overtone only (1st), raw spectra with T correction, 2nd overtone only (2nd), and 2nd derivative with T correction, 2nd overtone only (3rd). ....	32
Figure 5-1: Sample 20053365 placed over the integrating sphere of the FT-NIR Analyzer to determine its absorbance.....	35
Figure 5-2: Entire spectra of multiple mixtures of different amine loadings onto KCl. ....	38
Figure 5-3: Absorbance spectra for samples A, B, & C in the 5600-5900 cm <sup>-1</sup> . ....	38
Figure 5-4: Calibration model for the concentration obtained by using the spectra analysis on the 1 <sup>st</sup> overtone region to determine the ratio of the concentrations. Scales are unitless.....	39
Figure 5-5: Residual error plot of actual vs. predicted concentration for the spectra analysis of the 1st overtone to determine the ratio of the concentrations. Scales are unitless.....	40
Figure 5-6: Calibration model for the concentration obtained by using the spectra analysis on the 1st overtone region given the ratio between the two samples. Scales are unitless. ....	41
Figure 5-7: Residual error plot of actual vs. predicted concentration for the spectra analysis of the 1st overtone given the ratio between the two samples.....	42
Figure 6-1: Heated water vessel (left), and the flow through cell within the transmission module of the FT-NIR (right). ....	45
Figure 6-2: Lab setup of the inline monitoring system utilizing needle pumps for the injection of amine and HCl. ....	46
Figure 6-3: Raw absorbance spectra using the OMNIC software across the wavenumber region (4400 – 4258 cm <sup>-1</sup> ).....	48
Figure 6-4: A sample of the absorbance spectra against the examined region, 4400 – 4258 cm <sup>-1</sup> .49	
Figure 6-5: Normalized absorbance data for two slope regions vs. DoN. ....	50
Figure 6-6: Actual DoN vs. Calculated DoN for slope models developed after applying single-point normalization at 4331 cm <sup>-1</sup> . ....	51
Figure 6-7: Single-point normalization of the absorbance spectra at 4331 cm <sup>-1</sup> vs. wavenumber.51	

Figure 6-8: DoN vs area under the curve for points (4331-4258 $\text{cm}^{-1}$ ) after applying single-point normalization on the absorbance spectra. ....	52
Figure 6-9: Actual vs. Calculated DoN using the single-point normalization and area model with 95% C.I. ....	53
Figure 6-10: Absorbance for 1%, 2%, and 3% weight percent vs. the DoN at 4331 $\text{cm}^{-1}$ .....	54
Figure 6-11: Calculated vs. actual DoN using single-point normalization at 4331 $\text{cm}^{-1}$ . Data was divided to three separate figures to nullify the effect of weight percent on the absorbance. ....	55
Figure 6-12: Two-point normalization at 4331 $\text{cm}^{-1}$ & 4258 $\text{cm}^{-1}$ of the raw spectra. ....	56
Figure 6-13: DoN vs. slope (4400-4331 $\text{cm}^{-1}$ ) for two-point normalization model.....	57
Figure 6-14: Predicted DoN Vs. Actual DoN using the two-point normalization model. ....	57
Figure 6-15: Weight percent vs. DoN using a numerical model for 1 wt%, 2 wt%, and 3 wt%. ...	58
Figure 6-16: Calculated vs. actual DoN for 1wt%, 2wt%, and 3 wt% using Antaris software. ....	60
Figure 6-17: Residual error difference of the DoN data at 1%, 2%, and 3%.....	60
Figure 6-18: Calculated vs. Actual weight percent using the Antaris software.....	61
Figure 6-19: Residual error plot for the amine weight percent calibrated model using the Antaris software.....	61
Figure 0-1: 1 <sup>st</sup> overtone region of amine bond during the amine neutralization process. ....	69
Figure 0-2: 2 <sup>nd</sup> overtone region of amine bond during the amine neutralization process. ....	70
Figure 0-3: 3 <sup>rd</sup> overtone region of amine bond during the amine neutralization process. ....	70
Figure 0-4: Calibration model using the three amine overtone regions after smoothing filters were applied.....	71
Figure 0-5: Residual error plot using the three overtone regions of amine after smoothing filters were applied.....	72

## List of Tables

Table 4-1: Analysis type and overtones used vs. margins of errors produced.....	33
Table 5-1: Sample mixtures used to develop the calibration models.....	36

## **Abstract**

This work explores FT-NIR monitoring methods for Amine compounds commonly encountered in potash processing, including flotation reagents and their degree of neutralization, amine dosing in oils used as anti-caking agents, and loading analysis of anti-caking agents on solid product. FT-NIR was capable of accurately measuring amine weight percent in organic and aqueous solutions to within  $\pm 0.1$  and  $\pm 0.06$  wt%, respectively, and degree of neutralization during flotation reagent preparation within  $\pm 6\%$ . Mixing studies were also performed at industrially relevant conditions suggest that batch-to-continuous process retrofits of flotation reagent preparation units should consider the use of high-shear intensity mixers (i.e. orifice plates) over structured static mixing, with better dispersion observed in 1" Sch80 piping compared to 2" Sch80 piping.



## List of Abbreviations Used

DoN	Degree of Neutralization
FT-NIR	Fourier Transform Near Infrared
NH <sub>2</sub>	Amine
HCl	Hydrochloric Acid
NaOH	Sodium Hydroxide
PTAC	Part of the Amine Cycle
FT-IR	Fourier Transform Infrared
TOC	Total Organic Content
CMC	Critical Micelle Concentration
NaCl	Sodium Chloride
KCl	Potassium Chloride
CSTR	Continuously Stirred Tank Reactor
PVC	Polyvinyl Chloride
CPVC	Clear Polyvinyl Chloride
RMSEC	Root Mean Square Error of Calibration
RMSEP	Root Mean Square Error of Prediction
EN	Electronegativity
PFA	Perfluoroalkoxy Alkanes

## Chapter 1 Introduction

Long-chain fatty acids with amine functional groups are employed in the potash extraction industry as a flotation reagent during the selective separation of KCl from NaCl. During this process, the R-NH<sub>2</sub> functional group is neutralized to an R-NH<sub>3</sub><sup>+</sup> form which interacts with the defects in the KCl crystal, selectively binding to KCl and enabling air attachment within the flotation unit. NaCl, which does not interact with the amine functional group, is subsequently collected from the bottom of the flotation unit. The amine reagent concentration and degree of neutralization (fraction of amine functional groups in the R-NH<sub>3</sub><sup>+</sup> state) in these applications has traditionally been measured by titration or by utilizing Baume scale tests. Complete neutralization of the amine reagent is an essential conditioning preparation step that takes place before the flotation process starts. Batch conditioning is widely used throughout industries by mixing both the amine and the HCl solutions together [1].

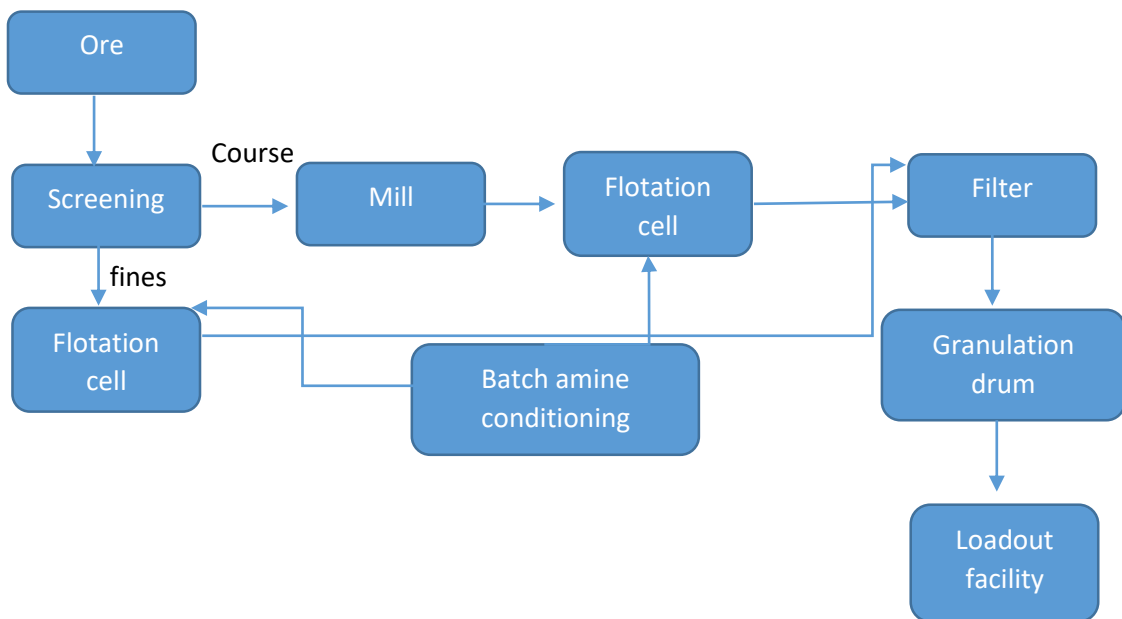


Figure 1-1: main unit operations of the potash extraction process.

Batch conditioning of the amine reagent has demonstrated a lack of homogeneity of the final solution. Due to mixing irregularities, complete protonation of the amine solution ( $R-NH_2$  to  $R-NH_3^+$ ) could not be achieved due to the formation of micelle globules that served as a protection layer against the protonation process [2]. Settling and separation of phases between amine solution and the aqueous solution has also been observed, leading to some concerns over fouling. As a result, there has been a gradual transition to continuous-based amine reagent preparation, for which limited information is available in literature on the degree of agitation required at commercially relevant flows to completely disperse injected amine into an HCl/water mixture.

Accurate monitoring of amine addition and neutralization is difficult to achieve through titration-based methods and pH due to an observed buffering effect from the amine solution. This is further complicated by routine drift of pH probes with time. Observed variations by as much as 5% and 8% from target amine dosing and neutralization have been observed in industry, which may increase amine usage or reduce subsequent flotation separation performance. Spectrophotometric-based methods are increasingly adopted due to their speed, simplicity of use, and relatively improved accuracy for a variety of applications. Fourier Transform Near Infrared, (FT-NIR), has significant spectral response to  $R-NH_2$  and organics, and has been used extensively as an industrial spectroscopy tool in a variety of applications. This thesis presents the development of monitoring methods for potash processing where the use of amines is predominant, specifically its preparation in the flotation reagent process as well as its use as an anti-caking agent during loadout, Figure 1-1.

This work focused on two aspects of the reagent preparation process; the mixing of the solution as well as its monitoring. Chapter 2 provides a brief review of spectrophotometric methods to establish common terminology and previous relevant applications to this work. Chapter 3 focuses on the mixing studies of batch-to-continuous conversion to examine multiple mixing elements to ensure a minimum of 95% degree of mixing of the amine across the column section. Chapter 4 examines the monitoring of amine dosing in oil and its respective absorbance through the FT-NIR analyzer, whereas chapter 5 studies amine monitoring as an anti-caking agent on solid salts and its absorbance. Once it was validated that the instrument was capable of determining the amine weight percent in these states, then a lab scale setup was put together to monitor the amine content and its degree of neutralization, (DoN). Chapter 6 combines the elements of chapters three, four, and five. It examines the reagent preparation of amine by ensuring continuous mixing as well as monitoring of both the amine weight percent and its degree of neutralization. Further, an inline setup was developed to ensure continuous monitoring of the solution as it passed through a flow-through cell implanted within the transmission module of the analyzer.

This thesis project has three main objectives. The first is to switch the overall process of the reagent preparation from a batch process to a continuous process and ensure dispersion of the amine solution takes place. The second objective is to look at the loadout facility, seen in Figure 1-1, and examine the use of FT-NIR to monitor the amine weight percent as both a control in liquid oil and as an anti-caking agent on solid KCl. The third objective is to develop an accurate, quick, non-hazardous, and continuous monitoring method to determine the weight percent of amine throughout and after the neutralization process.

These chapters are presented with the objective of enhancing the field of reagent preparation and process monitoring of amine solutions in the potash industry.

## Chapter 2 Review of Spectrophotometric Methods

There are a variety of methods for determining the concentration of amine in solution, differing in approach and accuracy. Many have accuracies limited to  $\pm 0.5$  wt% for amine determination, and require extended measurement times or sample preparation. This chapter attempts to provide a brief overview of common amine determination methods available in industry and published literature, specifically spectrophotometric methods.

Other spectrophotometric instruments have been developed in the oil industry to measure the concentration of amines as part of the amine cycle (PTAC). Some of these industries utilize the area under the peak as a procedural standard to determine the weight percent concentration, wt%. Process Raman spectrophotometric analyzer has been utilized to obtain the Raman intensity in which the peak ratios were then calculated [3]. A calibration curve was then developed from the peak ratios to determine the concentration [3]. These calibration models provided concentrations above 3.00 wt.% of the actual concentration [3]. The author also concluded that FT-IR provided similar results to that of the Raman analyzer, whereas the FT-NIR provided 50% more accurate results rather than both the FT-IR and the Raman analyzer [3].

Proton-transfer-reaction mass spectrometry is a monitoring technique that can be utilized to determine the concentration of amine solutions in the vapor phase [4,5]. The analytical technique employs hydronium ions, protons, as an ion source. The basis of this instrument is the measurement of the amount of hydronium ions that will react with the amine molecule. Through knowing the initial amount of hydronium ions present, the amount reacted with the amine, and the reaction kinetics of the amine molecule, one can determine how much of the amine was initially present. This analytical technique is helpful when the

affinity of the amine molecule is higher than that of water to the hydronium ion. This occurs when multiple functional groups are present to interact with the hydronium ions. This would lead to low reaction times and fast results without the need of calibration curves. However, most amines' affinity to the hydronium ion is lower than that of water. Under these circumstances, the method is not useful. Additionally, the duration of testing for each sample is highly dependent on the affinity. Some tests may take one second to provide a concentration magnitude while other tests may take 30 minutes.

Total Organic Carbon, (TOC), is an analytical method that is used to determine the concentration of amines. The method focuses on the hydrocarbon chain rather than the amine molecule itself. The TOC method involves the addition of an acid to oxidize the organic carbon and produce carbon dioxide. The formed carbon dioxide is then measured by a detector, and the amount of carbon dioxide measured is then related to the amount of organic carbon present in the sample. This technique requires that the reactions take place in the aqueous phase, suggesting that the technique is labor intensive and requires some preparations before the concentration is determined; hence this method can be replaced with a faster method that does not require any sample modifications [6]. TOC technique in fact requires a minimum of 4-6 minutes to complete a single measurement [6]. Dilution is also required with a factor of 2-50 depending on the type of reaction chosen [6]. A catalytic reactor would also be required for the oxidation reaction of the carbon. The second method is a quantitative method that involves a series of analytical tests [6].

FT-NIR in recent years has been used within many applications to measure the concentrations of many solutions and mixtures in all three states [7,8]. The instrument is known to provide absorbance measurements within a matter of seconds. The analyzer has

also been coupled with many mathematical and statistical techniques to provide first and second derivative analysis of large sets of spectra data [9]. This coupling of techniques has been applied to the pharmaceutical industry that focus on amine concentrations to measure protein densities as part of off-line and on-line sampling [10]. The analyzer has been used to carry out analysis to determine reaction kinetics of both heterogeneous and homogenous reactions in either liquid or vapor states [11]. Continuous or on-line monitoring of solution is discussed further in Fischer et al. applications [12]. Other spectrophotometric instruments have been developed in the oil industry to measure the concentration of amines as part of the amine cycle (PTAC). These two industries utilize the area under the peak to determine the weight percent. Process Raman spectrophotometric analyzer, a spectrophotometric instrument, has been utilized to obtain the Raman intensity in which the peak ratios were then calculated [3]. This instrument however has not provided accurate measurements [3].

Recent papers utilized both FT-IR and FT-NIR as the means to obtain the absorbance of amine-containing molecules. Pandita et al. utilized both FT-IR and FT-NIR to measure the absorbance of an amine-containing molecule [13]. The sampling was done out-of-line, and the absorbance of the amine band was obtained in the range of  $4935\text{ cm}^{-1}$ . Further, the experimental range of temperatures was within the range of this works' range as well, making it comparable to this thesis's work [13]. The temperature was also considered as it impacted the absorbance of the solution. Additionally, DeBakker et al. used FT-NIR to measure the absorbance of an amine-containing molecule [14]. Moreover, Abd El-Ghaffar et al. demonstrated the use of both FTIR and UV/vis in measuring the absorbance of Diethnaol amine [15]. The author also considered the impact of pH changes on the solution;



therefore, pH controlled experiments were conducted with buffer solutions at pH levels of 5, 7, and 9 in order to minimize any pH influence on results [15]. Furthermore, the analysis of the solutions was conducted in the range of 60-65° C [15]. The temperature range of the referenced work was within the preferable temperature range of this work's experiments.

The measurement technique utilized at Mosaic is titration-based in a laboratory setting. This makes the overall flotation process discontinuous. Therefore, this thesis focuses on integrating the continuous monitoring system with the process to determine the wt% of the amines. Further, the monitoring techniques will be utilized to measure the degree of neutralization of the solution. This helps in determining the amount of reagent to be added as well as enhancing the recovery. FT-NIR instrument will be utilized to determine the wt% as well as the degree of neutralization as part of a compact stream-based analytical instrument. This instrument can be installed in-line as part of a new continuous process without the need of sampling the solution and examining it in a lab-setting as currently employed. The spectrophotometric instrument will be calibrated to examine parameters such as optimum wavelength, and minimum flow rate requirement to avoid the precipitation of fatty amines inside the walls of the instruments and the tubes. These standards are the basis to developing a calibration curve that is capable of predicting the amine weight percent and its degree of neutralization.

## Chapter 3 Mixing Studies

### 3.1 Introduction

Potash processing involves the selective separation of KCl from NaCl, where a fatty acid amine is added to an aqueous slurry enabling preferential air-attachment to KCl during subsequent flotation. These amine molecules consist of a long chain fatty acid and a hydrophilic amine group which must be hydrolyzed to become active (i.e.  $R-NH_2 \rightarrow R-NH_3^+$ ). The resulting cationic amines are then capable of binding to the lattice defect present in KCl, enabling selective air-attachment and separation from NaCl.

The efficiency of this process is reliant on aqueous miscibility of the amine phase resulting from a high degree of neutralization (95%+) and the preparation of a homogeneous emulsion [16,17]. The critical micelle concentration, CMC, and aggregation of the emulsion is dependent on the concentration of HCl added during neutralization, where the CMC increases by 12.5% with HCl: Amine ratios from 0.1:1 to 1:1, and a 1:1 addition ratio of HCl to amine results in higher average molecular weights of the rod-like micelle in the absence of NaCl [18]. HCl molarity ratios greater than 1:1 resulted in increases in the aggregation number in the presence of NaCl, with higher ratios of HCl increasing the aggregation of the micelle globules even in the presence of low salt concentrations. During neutralization, a protective layer of micelles has been observed around globules of unreacted amine [19,20,21,22], where homogeneity cannot be achieved until these large micelle droplets breakdown and the non-protonated amine is made accessible. Protonation of the amine molecule has also been shown to be limited by diffusion into the agglomerate globules [23], increasing the importance of proper dispersion and breakup of amine during

the reagent preparation to ensure that length scales of globules are minimized and protective micelles do not inhibit neutralization.

Historical reagent production has involved either batch preparation or the use of CSTR's in series to generate a partially neutralized emulsion, after which storage in a day-tank allowed for the remaining neutralization to take place (Fig. 3-1) [17,24]. These methods are known to yield incomplete protonation of the fatty amines, increasing reagent usage and reducing the efficiency of downstream flotation [17,24]. The multi-tank arrangements also require significant space within operation facilities, and must be maintained at temperatures above the craft point to maintain the emulsion. The use of in-line mixing and batch-to-continuous design strategies has been pursued in the interests of process intensification and improved neutralization performance. Inline mixers have been utilized experimentally to increase the dispersion of both air and liquid flows [25,26,27,28]. In general, structured static mixers perform best at relatively low flow rates to enhance radial mixing [29]. Orifice plates have also been used as static mixers, forming jet streams that increase the mixing of aqueous solutions [30,31]. In similar applications, high energy dissipation breaks down the oil droplets and aids in the dispersion of the solution and homogenization [32,33]. As part of this strategy, water, HCl and heated reagent are combined and passed through either a static or active mixing element to disperse the emulsion and promote rapid neutralization. The performance of different mixing elements within this application had not previously been characterized.

In this work, the performance of four in-line mixing strategies is evaluated at industrially relevant reagent preparation conditions, such as flow rate and temperature, through video analysis of emulsion dispersion following amine injection. The mixing approaches

considered included inherent turbulence and an orifice plate within both 1” and 2” piping, and a commercially available 2” structured Koflo<sup>®</sup> mixer. The intent of this work is to guide the selection of suitable mixing techniques in future batch-to-continuous process conversions for reagent preparation.

### **3.2 Experimental Setup**

Mixing and dispersion experiments were carried out in a purpose-build flow loop (Fig. 3-1) capable of viewing the mixing and dispersion of injected media within a recirculated inventory. Flow in the system was maintained using a chemical resistant centrifugal pump (Laing Thermotech E10, 11.6gpm max flow rate), with the temperature controlled at set points ranging from 50 to 70°C using a flange-mounted 1500Watt screw-plug immersion heater (Tempco). The columns were constructed primarily of Sch80 CPVC pipe, with the exception of the injection and viewing areas comprised of clear PVC sized in accordance with each of the tests performed.

For each test, the recirculating system was initially filled with municipal water and heated to stable temperature above the craft point of the amine being tested. Based on the determined liquid inventory of a given mixing and piping configuration, HCl was added to the heated recirculating water such that, for the flow rate measured for each system, a stoichiometric molar flow rate of HCl to Amine would be present in subsequent injection testing. The solid amine was then melted on an external hot-plate and injected into the recirculating fluid using a metering pump (Cole Parmer 75211-30, equipped with Micro-pump P23 head). The rate of injection was established for each experiment to ensure that amine content and dispersion behavior downstream of the injection point would reflect industry-relevant conditions.

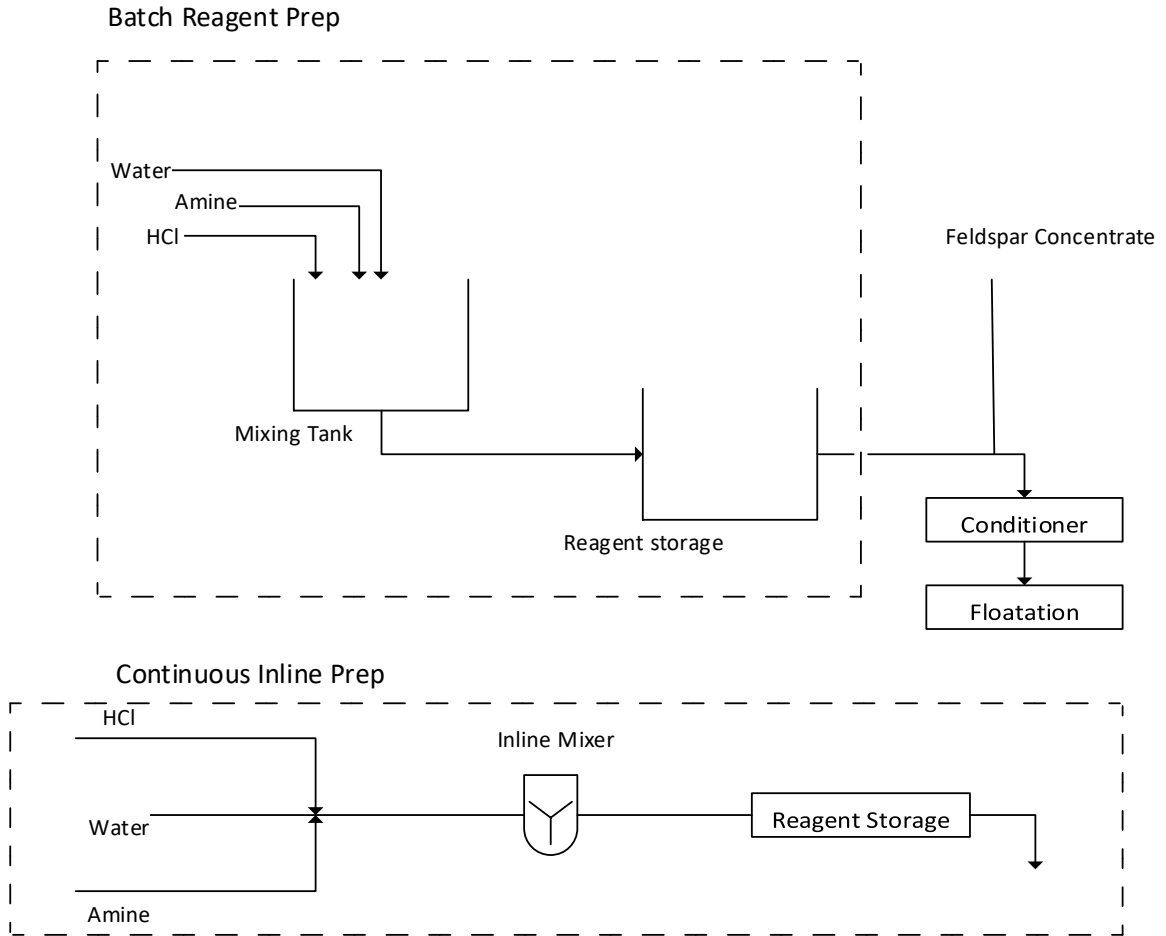


Figure 3-1 Schematic of the batch reagent preparation and the continuous inline preparation.

A total of five mixing configurations were explored, including 1” and 2” pipe with and without orifices located 6” downstream of the injection point, and a 2” pipe equipped with a commercial static mixer (Koflo 2-40C-4-6-2). The installed orifice in both systems was designed to result in comparable pressure drop to the Koflo static mixer at relevant flow conditions (approximately 2.5 kPa), resulting in a beta ratio for each orifice of ~0.7. The orifice was installed within the union located immediately after the injection point, with clear pipe installed following the union for flow visualization.

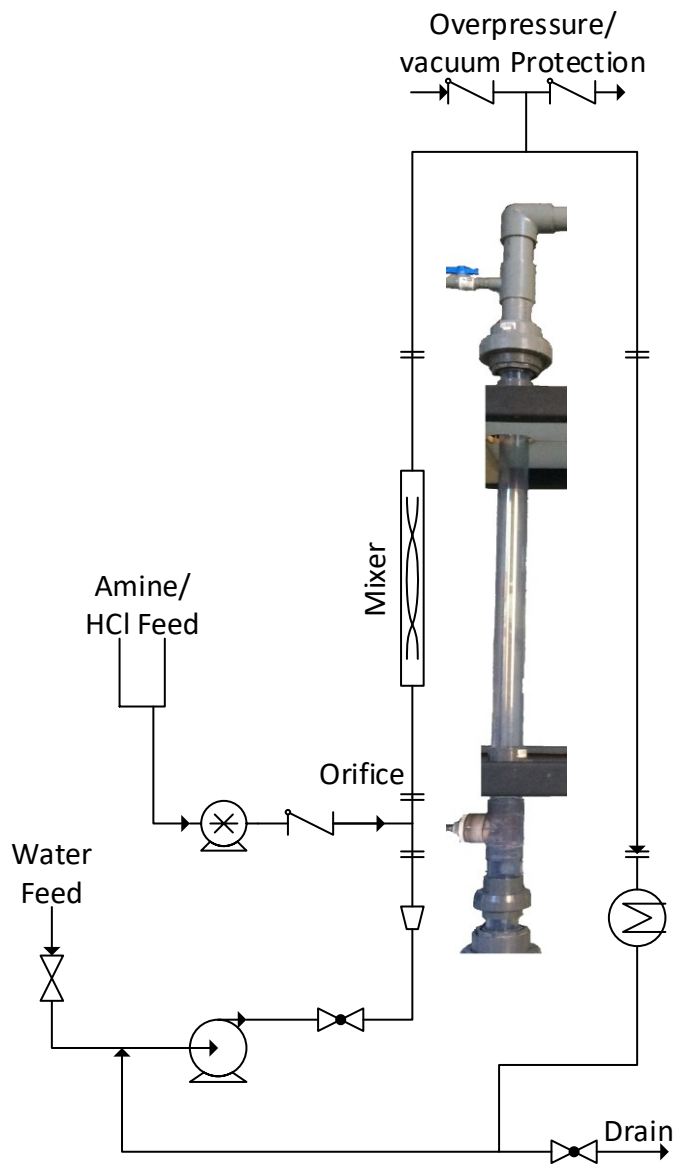


Figure 3-2: Schematic of the constructed flow loop with the vertical visualization region depicted (inset) for an empty 2” pipe downstream of the injection point.

The resulting dispersion patterns were recorded using a high-definition video camera (Panasonic HC-V500) for the duration of injection and initial stages of full recirculation of the media. During each experiment, the window for visualizing dispersion ranged from 12 to 20 seconds from initial injection time, after which recirculated media which had been completely sheared by the Liang thermos-tech pump re-entered the field of view. The

videos were subsequently analyzed using ImageJ to qualitatively and quantitatively assess the degree of dispersion observed.

### 3.3 Results & Discussion

For each of the mixing configurations tested and recorded, video post-processing was applied to better visualize the dispersion of injected media downstream of the injection point. This process was illustrated in Figure 3-2, with subsequent figures showing the specific results for each mixing configuration. Reflections and artifacts in raw videos were first minimized through background correction, where a 15-frame average of the HCl/water-filled column just prior to initial amine injection (Fig. 3-3a) was used as a baseline from which absolute deviations were determined (Fig. 3-3b, black prior to injection). During injection, amine in the column appears as lighter regions, with intensities still varying with position depending on residual reflections (Fig. 3-3c).

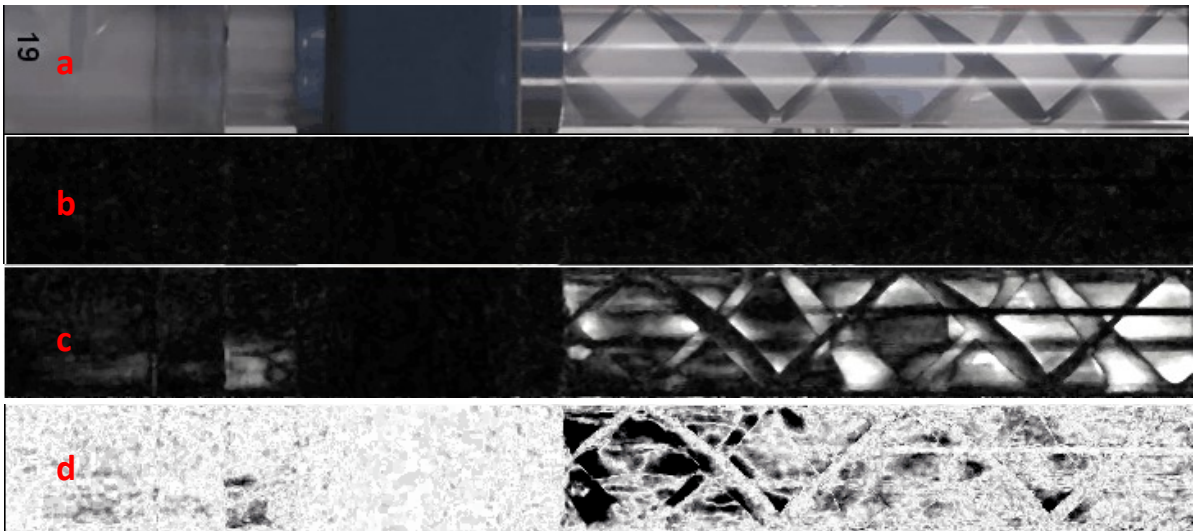


Figure 3-3: Illustration of post-processing method applied to videos captured for each mixing configuration. Raw (a), background corrected at pre-injection (b) and injection conditions (c), and normalized variation during injection (d).

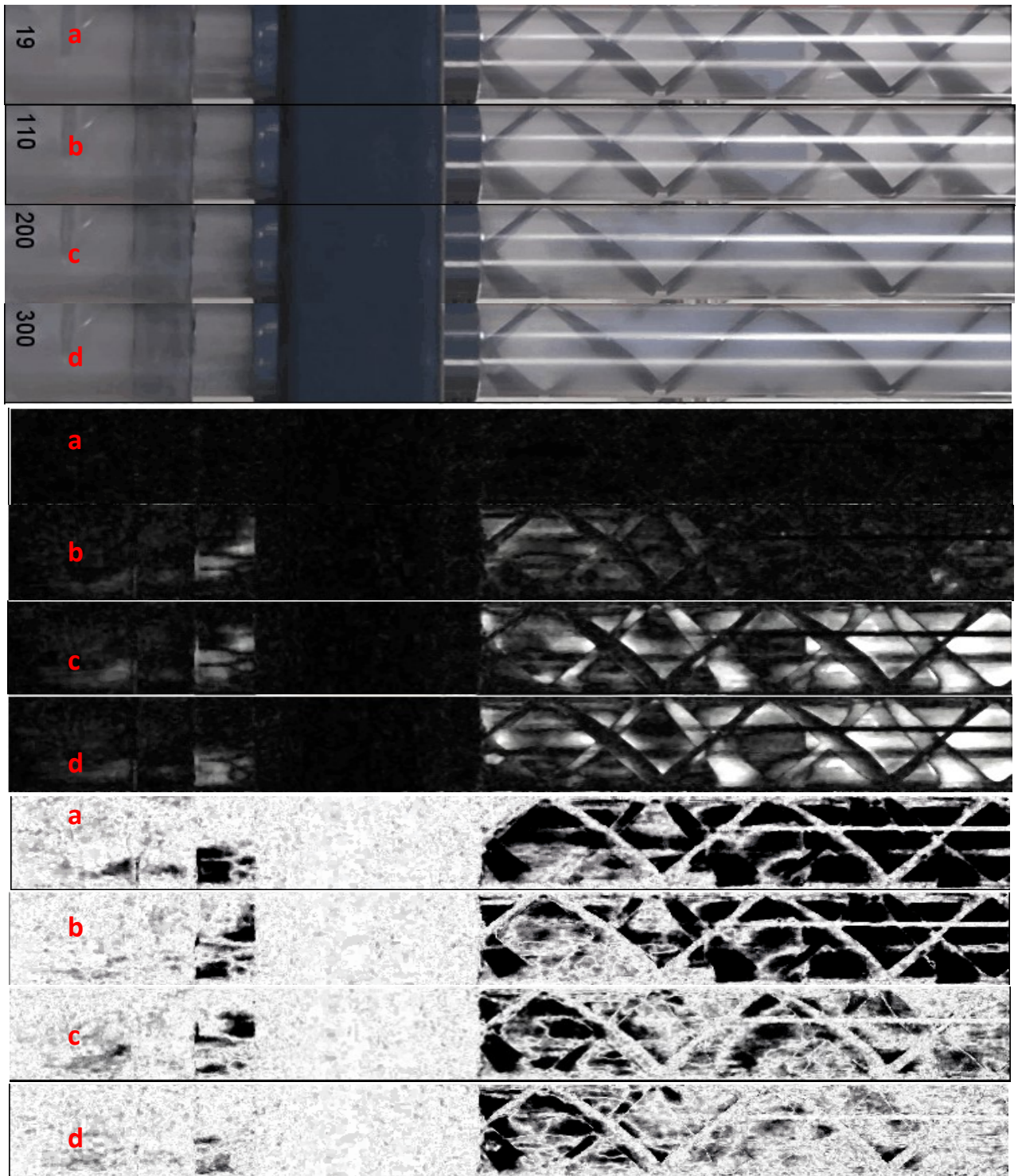


Figure 3-4: Amine injection into a 2" Koflo mixer: raw images (top), background corrected (middle) and variance normalized (bottom). Background corrected images appear white as amine is injected, while variance normalized images appear white as the column appearance approaches that of well-dispersed conditions.



These images were then normalized, where white pixel values correspond to images consistent with the appearance of the column following complete recirculation. The resulting normalized variation images (Fig. 3-3d) provided a quantitative method of assessing the dispersion of amine within each mixing configuration through comparison to recirculation conditions where dispersion is complete. Note that this normalization method did not necessarily result in a uniform black image at pre-injection conditions. Even with background correction, variations in the reflections between pre and post injection conditions did create some initial normalized intensity.

A primary conclusion which was drawn from this work was that a single, in-line active mixing device (such as the pump used here) was sufficient to ensure complete dispersion of the amine solution. However, given the inherent power requirements associated with active mixers, passive mixing strategies were preferred.

The dispersion of amine within the 2" Koflo mixer (Fig. 3-4-bottom) increased with each mixing element in series (Fig. 3-5). Injection into this system was achieved through a 1/4" stainless tube protruding into the center of the flow path, where momentum from the injection port resulted in a bias of the amine plume towards the right side of the column as pictured (white regions in Fig. 3-4, middle images). By the 5<sup>th</sup> mixing element, 80-85% dispersion was achieved relative to fully recirculated conditions. A minimum of six elements were required to achieve the maximum dispersion possible given this configuration and the turbulence it produced, suggesting that a 12-element mixer or a smaller dimension device may be more suitable for this application.

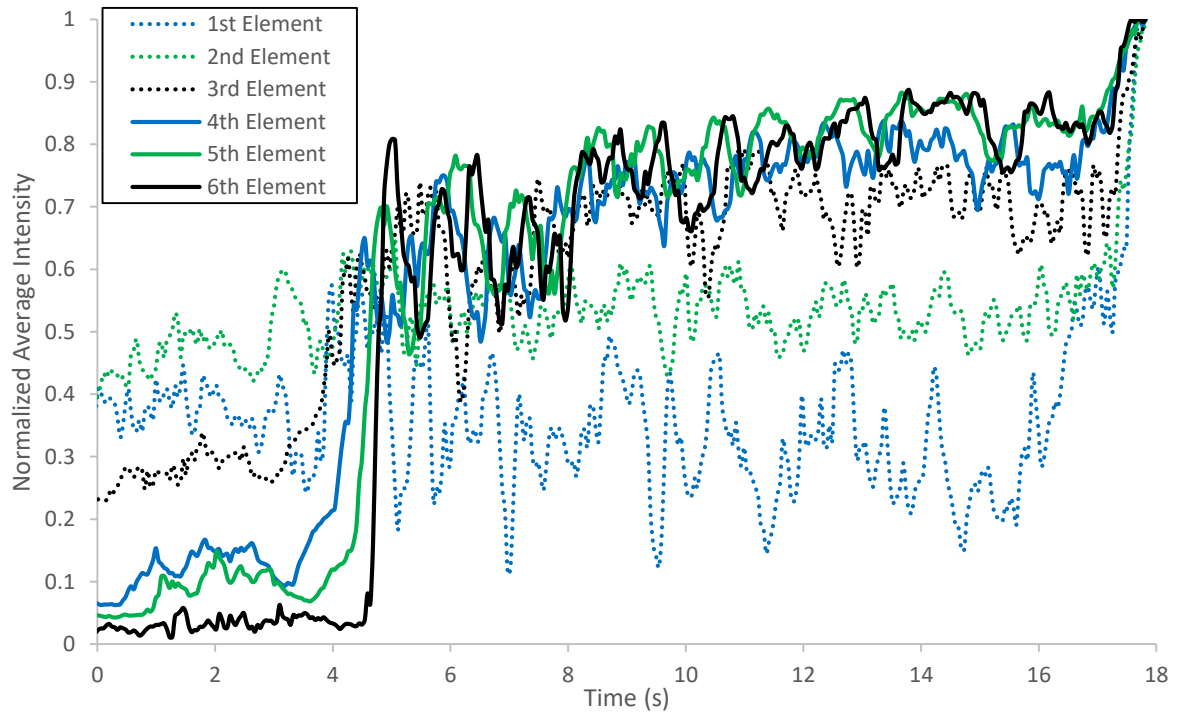


Figure 3-5: Normalized average intensity vs position (mixing element) within the 2” Koflo mixer during injection. Note that at  $t \sim 18$  seconds full recirculation occurs and all intensities approach 1.

The Reynolds number for the 2” pipe and flow conditions tested ranged from 15,000 to 20,000, which were well within the turbulent flow regime where natural dispersion was considered a viable possibility. Experiments were thus carried out without any form of mixing through a 2” clear PVC pipe replacing the Koflo mixer (Fig. 3-6), where images at  $t=20$  seconds illustrated the column contents after complete recirculation had occurred.

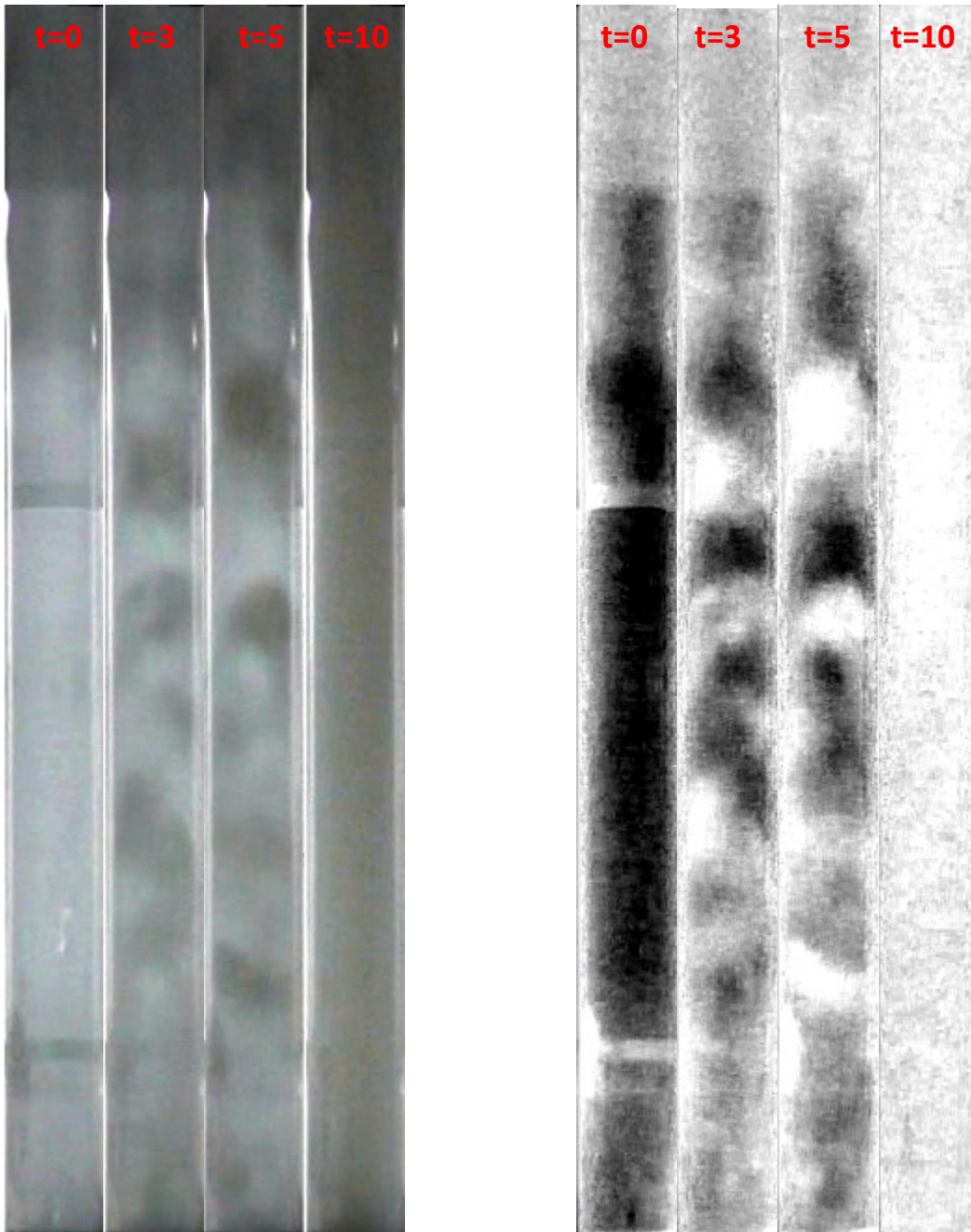


Figure 3-6: Amine injection into a 2" pipe with no mixing element or orifice: raw images (left) and variance normalized (right). Flow is in the upward direction.

During injection, significant slugging is observed within the column with the amine failing to naturally disperse across the column cross-section. While downstream fittings and flow path deviations would likely help to complete the dispersion process, this amine is known

to adhere to and build up on vessel internals and is desired to be dispersed as quickly as possible. Relying on natural turbulence within a 2" process line failed to produce an acceptable level of dispersion following injection, confirming the need for some form of downstream mixing element. The impact of introducing a mixing orifice plate 6" downstream of the amine injection point was thus explored as a more economical alternative to a structured static mixing device. The plate used was designed to produce a pressure drop of ~2.5kPa, comparable to the pressure drop of the Koflo mixer at these conditions. The orifice plates had beta coefficients of 0.7. The resulting dispersion of the injected amine was nearly complete (Fig. 3-7), with a wave of dispersed amine travelling up the viewing area following initial injection and a column appearance approaching that of completely recirculated media during normal injection.

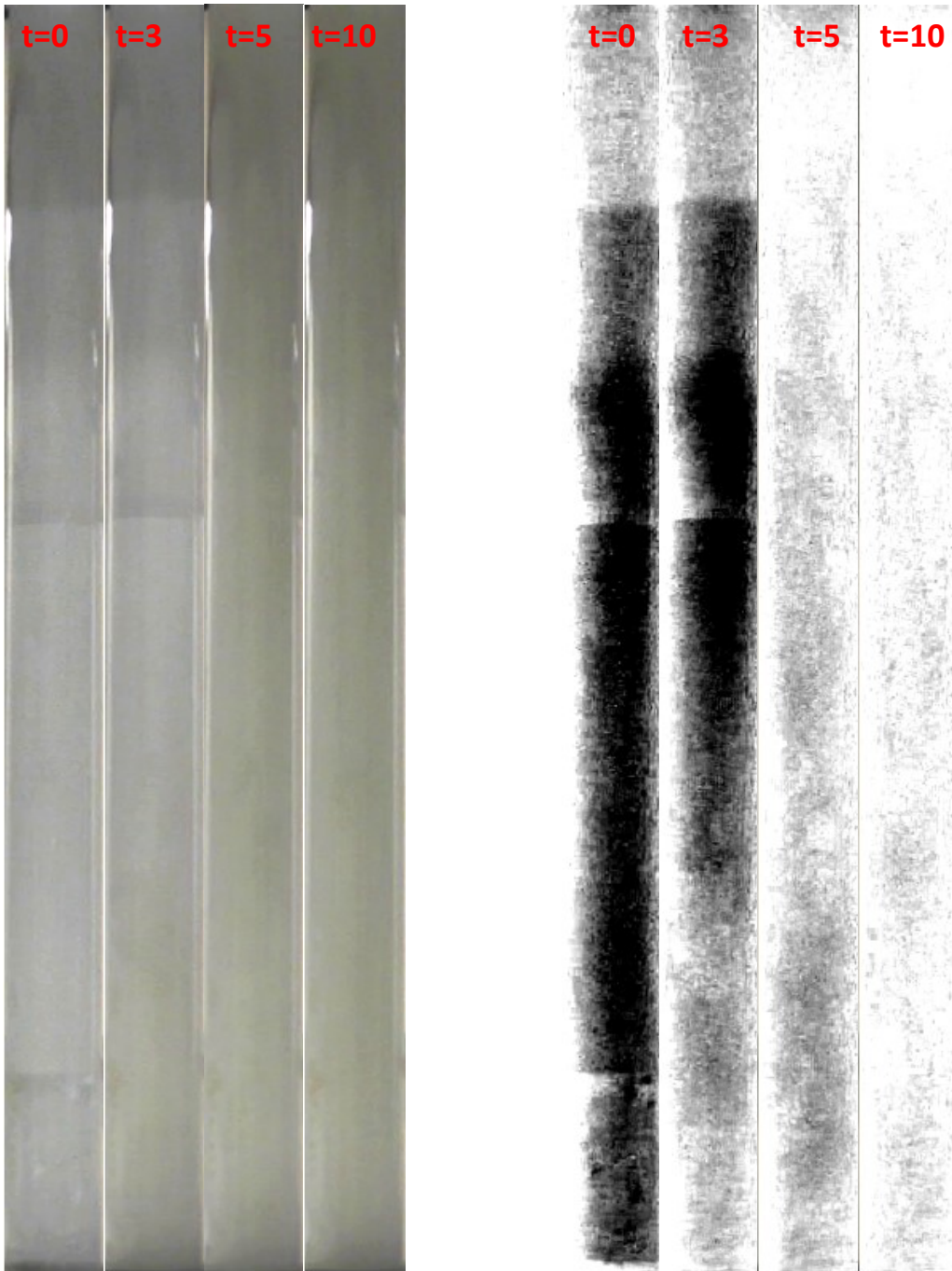


Figure 3-7: Amine injection into a 2" pipe with an orifice ( $\beta=0.7$ ): raw images (left) and variance normalized (right). Flow is in the upward direction.

In comparing the average normalized intensities for these three mixing approaches within the 2" system (Fig. 3-8), the use of an orifice plate was able to generate a more uniform dispersion than was observed in the final mixing elements of the Koflo mixer (element 6,

Fig. 3-5), suggesting that for this specific application a single, point-source of energy dissipation was more efficient than a repeated structured packing approach. Note that in Fig. 3-8, a drop in the normalized intensity is observed for both the empty column and orifice testing at times ranging from 10 to 12 seconds. A smaller reservoir of amine was employed in these tests to more clearly define the injection phase (left side) from the onset of recirculated media (right side).

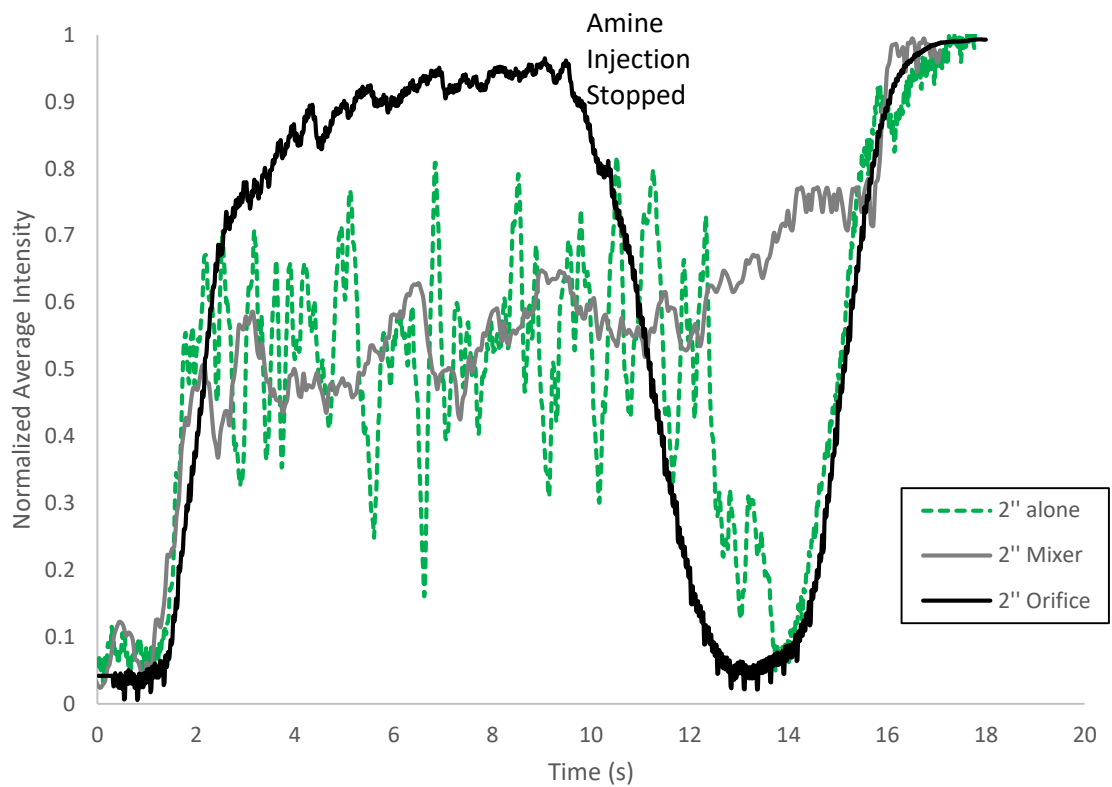


Figure 3-8: Normalized average intensity vs time for the 2” configurations. Note that amine injection was stopped at 10s and 12s for the orifice test and “alone” test, respectively. Continuous amine injection was performed for the system using the Koflo mixer.

For industrially relevant conditions, a reduction in line size to 1” was considered feasible for reagent preparation, where the increase in Reynolds number (up to ~35,000) could improve natural dispersion. Two additional experiments were carried out to explore the

relative efficiency of injection into an empty 1” process line and injection into the same system with an orifice plate ( $\beta=0.7$ , located 6” downstream of the injection point). The relative normalized variance images were subject to increased reflections and artifacts due to the higher radius of curvature of the tubes (Fig. 3-9). When expressed as a normalized average intensity (Figure 3-10), the orifice continued to exhibit excellent dispersion performance while the empty 1” pipe still failed to fully disperse the amine despite the increased free stream turbulence.



Figure 3-9: Variance normalized images during amine injection into a 1" pipe without (left) and with (right) and orifice plate present ( $\beta=0.7$ ). Flow is in the upward direction.



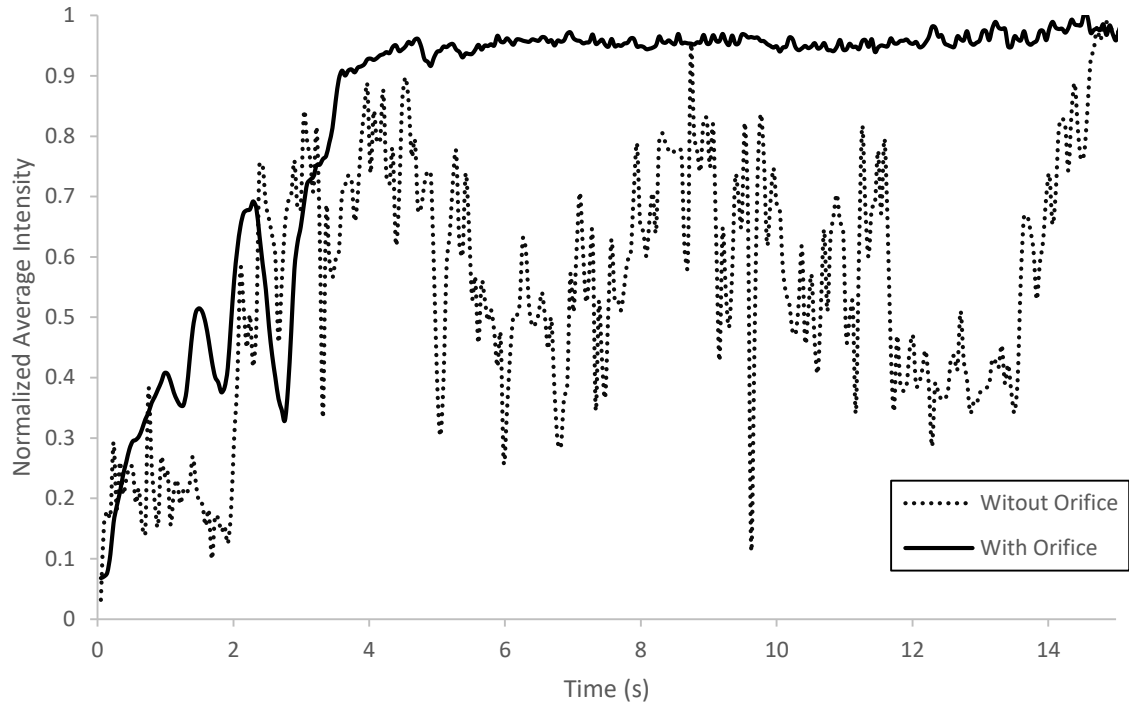


Figure 3-10: Normalized average intensity vs time for the 1” pipe configurations with and without an orifice present.

### 3.4 Conclusion

Dispersion behavior was observed in both 1” and 2” lines without an orifice, with an orifice, and a 2” line with a static mixer. For each of the line sizes, the use of an orifice with  $\beta=0.7$  was sufficient to fully disperse the injected amine, suggesting that a single-point for energy dissipation was more effective in preparing a consistent reagent than the gradual dispersion observed in a more structured static mixer configuration. For an empty pipe, the free-stream turbulence present at these conditions was not sufficient to breakup and disperse the injected amine within the viewing region observed. While it is possible that downstream flow deviations would assist in this process (especially within the 1” line), failure to fully disperse the amine following injection could lead to accumulation on the pipe surface and the need for increased maintenance over time.

## Chapter 4 Liquid Amine Monitoring in Oil

### 4.1 Introduction

Armeen T, a long carbon chain amine molecule, is utilized as a chemical intermediate, a mineral coating, an anticaking additive, and as a hydrophobe building block. In anticaking applications, the amine molecule must be added to the final product, KCl, at a certain weight percent in order to be accepted by the clients. The acceptable weight percent of Armeen T is in the range of 0-7 wt%. Neither titration based techniques nor Baume scale can provide measurements within a 0.1% margin of error. Therefore, Fourier transform near infrared, (FT-NIR), is explored as a measurement with sufficient accuracy for online process monitoring. The Antaris II FT-NIR, seen in Figure 4-1, is a spectrophotometric instrument that utilizes the distinctive vibrations of bonds and measures their absorbance at their respective wavelengths. FT-NIR is utilized as it covers a wide range of wavelength numbers,  $10,000-4,000\text{ cm}^{-1}$ , and can specifically distinguish R-NH<sub>2</sub> bonds.

The amine weight percent can be calculated through utilizing a calibration curve that is obtained from the FT-NIR system. For R-NH<sub>2</sub>, three overtone regions were observed in the standard calibration range tested (Figure 4-2). These overtones represented vibrations of the amine bond at its respective wavenumber. Of these regions, the first overtone region is susceptible to interference from water and possibly the oil present for dilution, so only the second and third overtone regions were explored in detail.

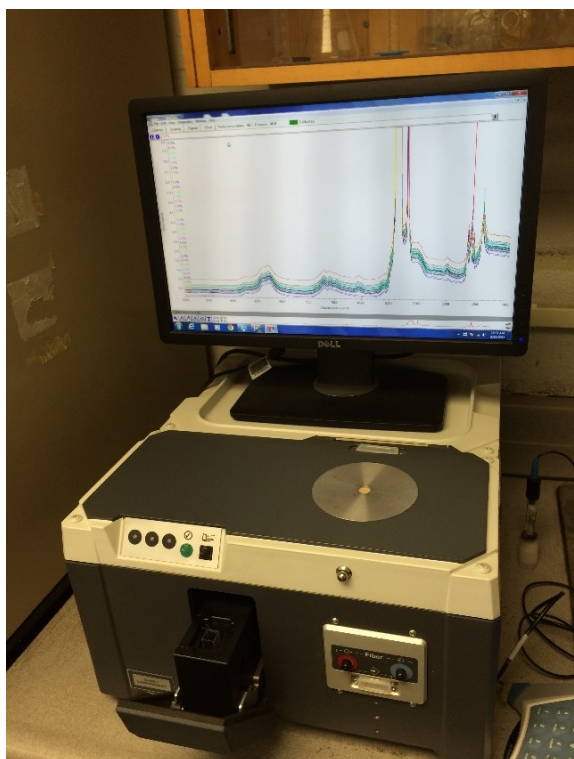


Figure 4-1: ThermoScientific FT-NIR

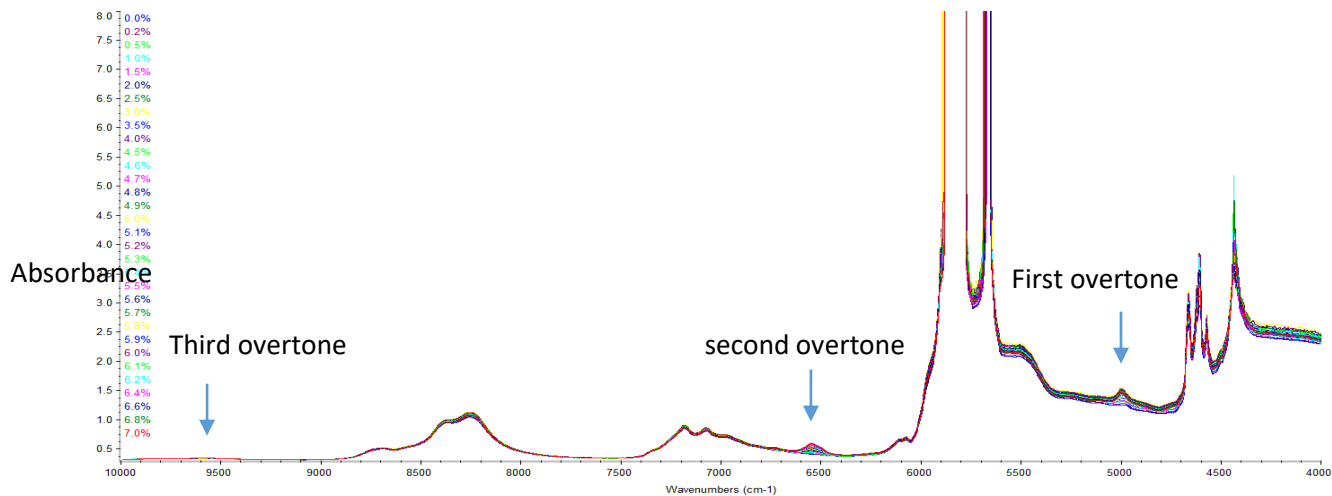


Figure 4-2 : The entire spectra of the solution for various amine wt% concentrations

## 4.2 Experimental Procedure

The experiment involved the addition of Armeen T to a light oil at set dosing rates. The amine/oil mixture temperature was maintained at 40, 50, and 60 °C, which was sufficient to maintain the Armeen T in its liquid state. A 1 cm path length quartz cuvette was utilized in the transmission cell of the FT-NIR instrument in order to measure the absorbance. A background sample of the empty light path was initially taken to ensure that any environmental changes within the lab were accounted for in the sample spectra. In total, 50 samples were taken in which 40 were used for calibration model development and 10 were used for validation. Subsequent to model development, additional batches were prepared and examined against the calibration to determine the applicability of the calibration graph. For each sample measurement, 15 scans were collected with a resolution of 8  $\text{cm}^{-1}$  in 10 seconds. The amine bond presented itself in the first ( $\sim 5000 \text{ cm}^{-1}$ ), second ( $\sim 6700 \text{ cm}^{-1}$ ) and third ( $\sim 9700 \text{ cm}^{-1}$ ) overtone regions (Figure 4-2).

The second and third overtone regions were selected for analysis due to the presence of distinct and visible peaks for the  $\text{NH}_2$  bond with an absorbance below a magnitude of 1. The 1<sup>st</sup> overtone region was also distinct and visible, but since the absorbance magnitude for the 1<sup>st</sup> overtone was 1 to 2 (i.e. 90 to 99%) and could potentially experience interference from the organic spectra of the oils, it was not used. The spectra were also processed using a 1<sup>st</sup> derivative analysis as it accounted for shifts in total absorbance, providing a degree of background correction. The performance of quantification based on the raw spectra and 2<sup>nd</sup> derivative spectra were also analyzed and presented within this report.

A partial least square model was selected for the analysis of the amine/light oil mixture, with a Savitzky-Golay filter for smoothing. The second overtone region had a wavenumber

range of 6700-6390  $\text{cm}^{-1}$  while the third overtone region had a wavenumber range of 9780-9381  $\text{cm}^{-1}$ . Magnified spectra in the two regions are provided in Figures 4-3 and 4-4.

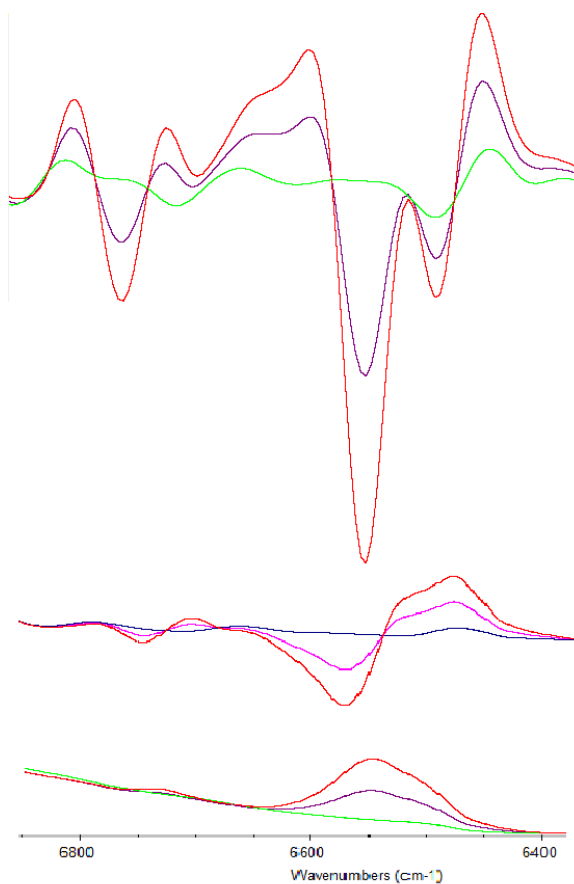


Figure 4-3: Top to bottom: 2<sup>nd</sup> derivative, 1<sup>st</sup> derivative, and raw spectra of the second overtone.

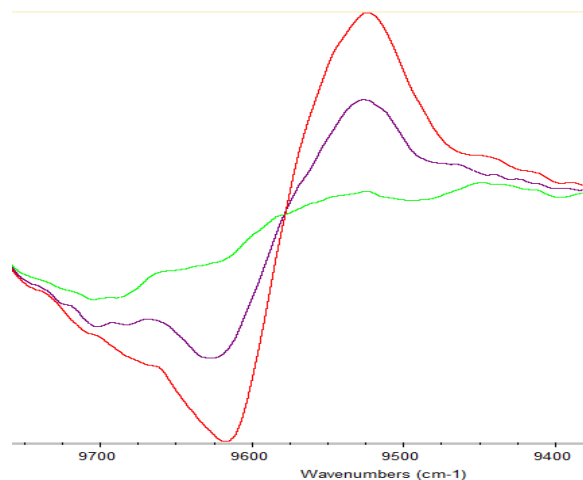


Figure 4-4: First derivative of the third overtone.

### 4.3 Results & Discussion

Calibration models were subsequently developed using the TQ Analyst software for the first-derivative of the spectra with temperature corrections included, yielding an equivalency plot (Figure 4-5) and error residual plot for the range of experimental conditions tested (Figure 4-6). The calibration model yielded a cross-validation factor of root mean square error of calibration, (RMSEC), of 0.0445 and an independent validation factor of root mean square error of prediction, (RMSEP), of 0.0333. The correlation coefficients of both factors were 0.9999, suggesting an excellent fit of the validation points to the calibration curve with an average margin of error of +/- 0.1 wt%.

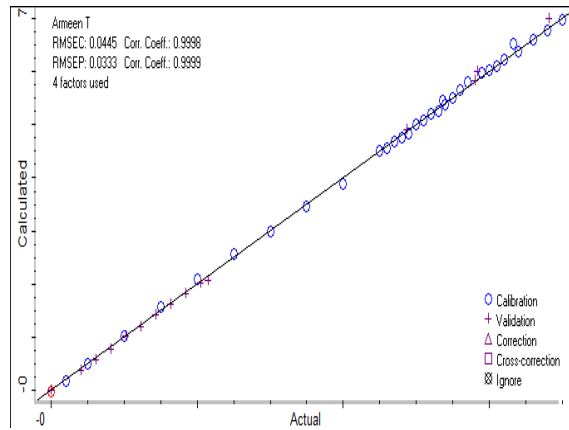


Figure 4-5: Calibration plot for R-NH<sub>2</sub> with temperature effect included.

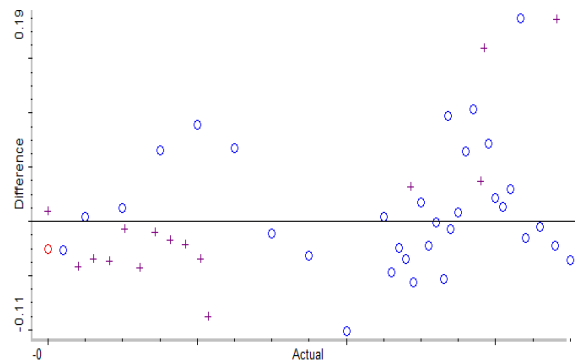


Figure 4-6: Residual error plot of actual vs. predicted for the 1<sup>st</sup> derivative analysis of the 2<sup>nd</sup> and 3<sup>rd</sup> overtones.

The calibration curve was obtained using four partial least square, (PLS), factors. The predicted residual sum of squares, PRESS, plot in figure 4-7 demonstrated that only one factor was needed. However, three factors were added to improve the correlation coefficients of the calibration curve from 0.9987 to 0.9999. This procedure provided an amine weight percent with a margin of error of +/- 0.1 wt%. Note that the potential to use a single factor for the determination of Armeen T content may offer the option to perform single wavelength absorption measurement for quantification.

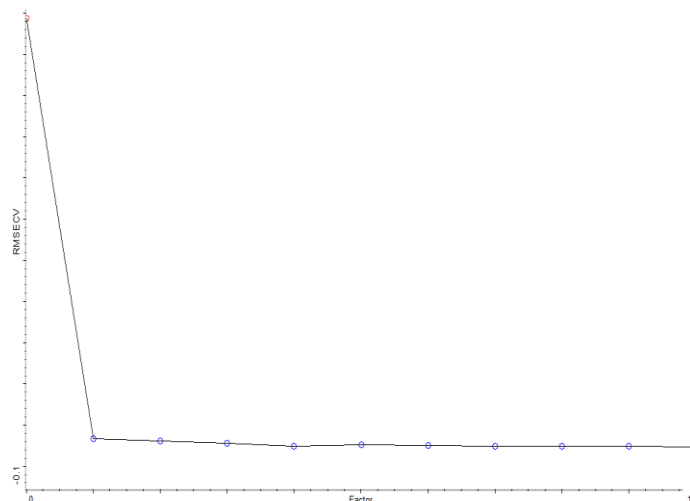


Figure 4-7: PRESS plot for Armeen T in light oil.

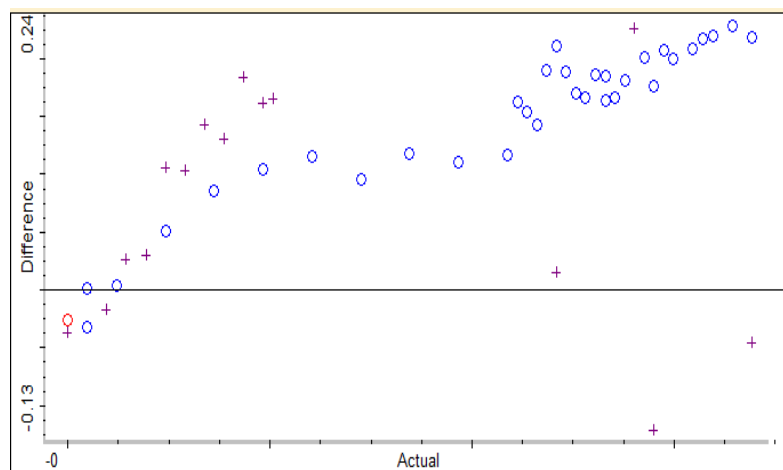


Figure 4-8: Residual error plot for 1st derivative spectra of both the 2nd overtone and 3rd overtone without the temperature correction included.

As the data points were taken at different temperatures, a temperature correction factor offered by the TQ Analyst program was applied. Temperature impacts the characteristic behavior of the R-NH<sub>2</sub> bonds. Increases in temperature led to decreases in the amount of light absorbed. Therefore, correction factors were applied to counter the temperature's effect. The residual error from the same data set without temperature correction is seen in Figure 4-8.



Three types of analysis, spectra, 1<sup>st</sup> derivative, and 2<sup>nd</sup> derivative, were also explored. These three analysis were tested against each other in order to determine the variability in prediction performance based on error residual plots (Figure 4-9). The three analysis types primarily focused on the second overtone region.

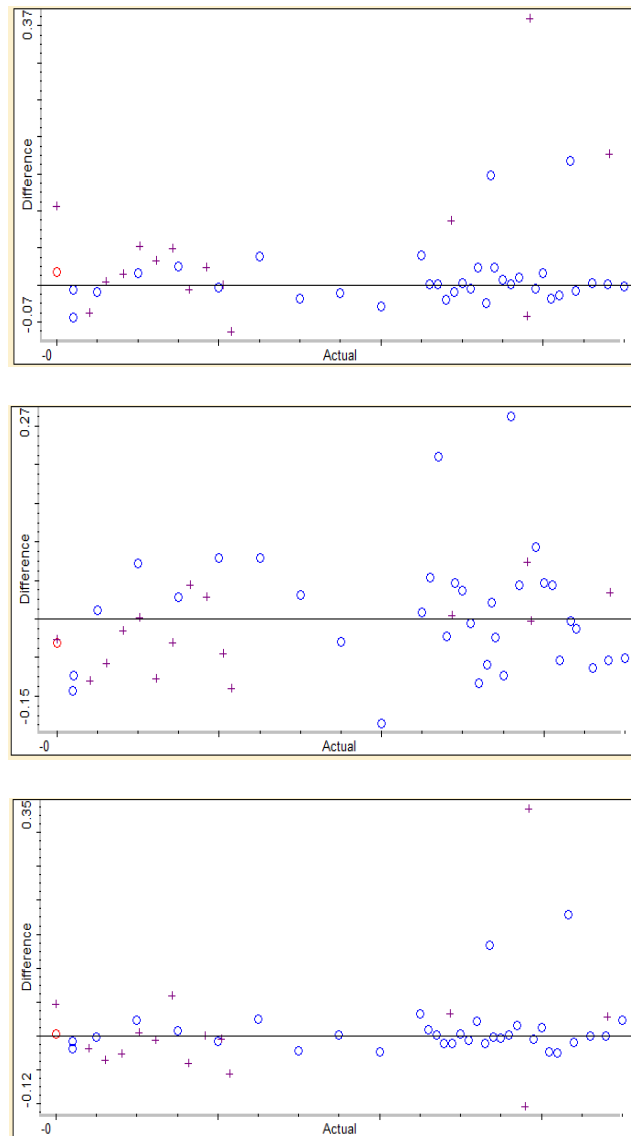


Figure 4-9: Residual error plots of 1st derivative with T correction, 2nd overtone only (1st), raw spectra with T correction, 2nd overtone only (2nd), and 2nd derivative with T correction, 2nd overtone only (3rd).

As seen in Table 4-1, the correlation coefficients were close to 1 for all spectral analysis approaches incorporating temperature correction. While use of the 2<sup>nd</sup> overtone alone did produce excellent measurement accuracy, the inclusion of the 3<sup>rd</sup> overtone region eliminated some of the remaining outliers.

#### 4.4 Conclusion

Fourier transform near infrared, FT-NIR, was successfully applied to quantify Armeen T content from 0 to 7% within light oil at temperatures from 40 to 60°C. While the use of the 2<sup>nd</sup> overtone provided good results, inclusion of the 3<sup>rd</sup> overtone is recommended due to its improved performance at higher wt% values. A temperature correction was needed, eliminating non-linear behavior of the data across the tested temperature range. The final calibration model using the 1<sup>st</sup> derivative spectra had a correlation coefficient approaching 1, and a performance index of 98.3. This performance index was the highest amongst all five different analysis types explored

Table 4-1: Analysis type and overtones used vs. margins of errors produced.

Analysis Type	Correlation Coefficient	Overtones used	Temperature Correction	Factors used	+ve error margin	-ve error margin
1 <sup>st</sup> derivative	0.9561	2 <sup>nd</sup> and 3 <sup>rd</sup>	No	4	0.24	-0.14
1 <sup>st</sup> derivative	1	2 <sup>nd</sup> only	Yes	4	0.37	-0.07
Raw Spectra	0.9991	2 <sup>nd</sup> only	Yes	2	0.27	-0.15
2 <sup>nd</sup> derivative	1	2 <sup>nd</sup> only	Yes	6	0.38	-0.12
1 <sup>st</sup> derivative	1	2 <sup>nd</sup> and 3 <sup>rd</sup>	Yes	4	0.19	-0.11

## **Chapter 5 Solid NaSt. weight percent monitoring**

### **5.1 Introduction**

Anti-caking agents are additives that prevent the aggregation of KCl crystals which may form cakes during transport. Cake formation results in difficulties in packaging, transportation, and handling of the salt, KCl. Therefore, the anti-caking agent was added in the industries to ease the overall process and prevent cake formation. The current techniques in determining the amount of the agent added include total organic carbon, (TOC), and wet chemistry analysis. The TOC method involves the addition of an acid to oxidize the organic carbon and produce carbon dioxide. The formed carbon dioxide is then measured by a detector. The amount of carbon dioxide measured is related to the amount of organic carbon present in the sample. This technique requires that the reactions take place in the aqueous phase, suggesting that the technique can be replaced with a faster method. TOC technique in fact requires a minimum of 4-6 minutes to complete a single measurement. Dilution is also required with a factor of 2-50 depending on the type of reaction chosen. Further, a catalytic reactor would also be required for the oxidation reaction of the carbon. The second method is a quantitative method that involves a series of analytical tests. Wet analytical chemistry may include titration which is a subjective method that requires a lab analyst to qualitatively determine when the color changes. Hence, a new method to measure the loading concentration of the anti-caking agent is explored. The explored method's advantages are that the measurement can be done within few seconds, no change of phase, no addition of acids will be required, and no dilution of the samples will be required.

Fourier transform near-infrared analyzer will be utilized to determine the ratio of one treated sample to another. Since the anti-caking agent contains an amine molecule, then the focus will be on the first overtone of the R-NH<sub>2</sub> bond. There will not be other molecules present, such as water, to impact the absorbance spectra within the first overtone region. The examined wavelength number will be between 10,000-4,000 cm<sup>-1</sup> with a special focus on the region 5,500-6300 cm<sup>-1</sup> as it contains the first overtone for the -NH<sub>2</sub> bond.

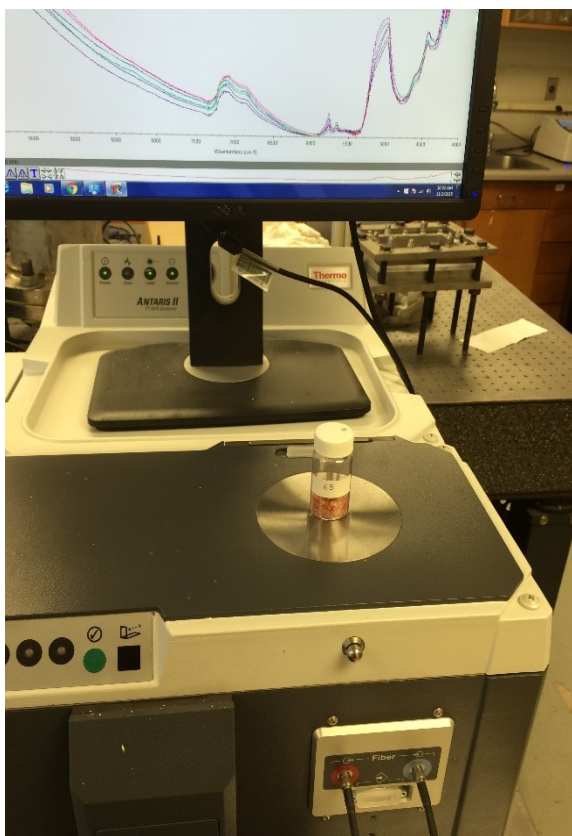


Figure 5-1: Sample 20053365 placed over the integrating sphere of the FT-NIR Analyzer to determine its absorbance.

## 5.2 Experimental Setup

Three samples were provided by Mosaic Inc. This work is done in agreement with them to enhance their monitoring of their amine loadouts. An untreated sample referred to in this

document as sample A, a sample with the code 20053371, sample B, and a sample with the code 20053365, Sample C. The main objective of this experiment was to determine the ratio of the added amount of the anti-caking agent to both samples B and C.

The FT-NIR analyzer was utilized to obtain the absorbance of all samples. Further, additional samples were created by mixing combinations of samples A, B, and C together.

Table 5-1: Sample mixtures used to develop the calibration models.

Name	Mass of A (g)	Mass of B (g)	Mass of C (g)
A	1	0	0
B	0	1	0
C	0	0	1
(xA, xB)	1	1	0
(xA, xC)	1	0	1
(xB, xC)	0	1	1
(xA, 2xB)	1	2	0
(xA, 0.5xB)	1	0.5	0

The samples were inserted into clear glass vials before they were put over the integrated sphere module. In total, 15 scans were collected for each sample with a resolution of  $8 \text{ cm}^{-1}$  in 10 seconds. A background reference was also collected before the beginning of the experiment to ensure that any environmental changes within the lab were accounted for in the sample spectra. On average, 10 spectra were collected for each sample to ensure that the samples were homogenous. This provided 50 spectra in total, in which 42 spectra were

used to develop a calibration model while the remaining spectra were used for validation purposes. Subsequent to model development, additional vials were prepared to ensure consistency within the absorbance for samples that possess the same composition. The main focus of the spectra was on the first overtone region ( $\sim 5600\text{ cm}^{-1}$ ).

Since the absorbance of the samples were expected to be less than 1, then utilizing the first overtone of the amine bond was viable. This assessment was due to the lack of presence of the  $\text{-OH}$  bonds which would have increased the absorbance over the value of 1.

The spectra were processed using the spectra analysis on the TQ Analyst software. The performance of quantification based on the 1<sup>st</sup> derivative and the 2<sup>nd</sup> derivative were not utilized since the spectra data provided a region with visible and distinct peaks. The spectra were analyzed using a partial least square model for the anti-caking agent/salt mixture. No smoothing filters were used on the spectra since the spectra did not possess any sharp edges within the region of interest, the first overtone.

The main objective of the first experiment was to determine whether or not FT-NIR can be utilized to determine the ratio between the two samples. The second experiment was a continuation on the first experiment. As the exact concentrations were provided by Mosaic Inc., the analyzer was utilized to develop a calibration model between the actual known concentrations and the predicted ones.

### **5.3 Results & Discussion**

The spectra were utilized to develop a calibration model. The entire spectra can be seen in Figure 5-2. The first overtone of the anti-caking agent's  $\text{R-NH}_2$  bond was present in the region  $5600\text{-}5900\text{ cm}^{-1}$ .

The calibration model was developed by utilizing the TQ Analyst software. The region of interest, Figure 5-3, had distinct peaks that made the spectra a viable reference to develop the calibration model.

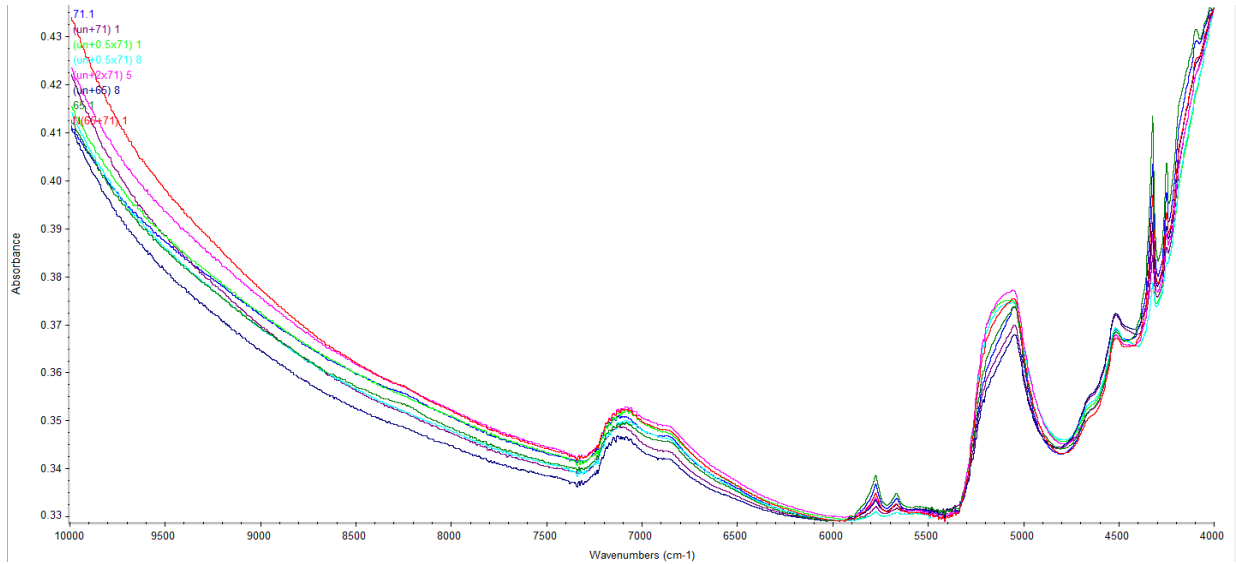


Figure 5-2: Entire spectra of multiple mixtures of different amine loadings onto KCl.

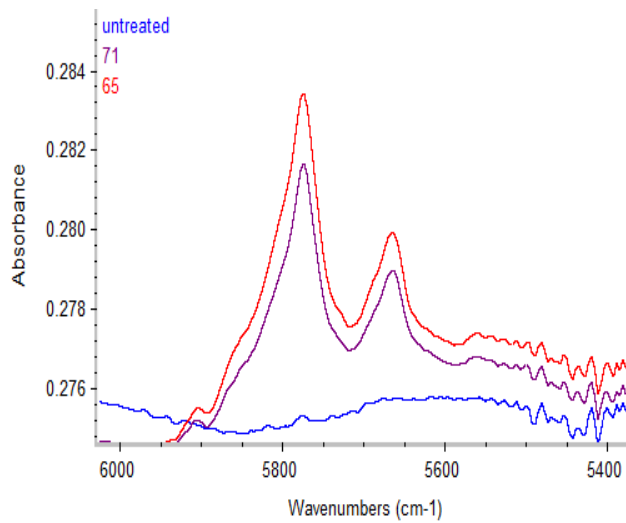


Figure 5-3: Absorbance spectra for samples A, B, & C in the 5600-5900  $\text{cm}^{-1}$ .

By utilizing this region, a calibration model was developed, figure 5-4. The calibration model yielded a cross-validation factor, RMSEC, of 0.474 and an independent validation, RMSEP, of 0.707. the correlation coefficients of both factors, 0.9904, and 0.9701

suggested a good fit of the validation points to the calibration model. The RMSEC and the RMSEP values were extremely high due to the presence of multiple data points at the same concentration. If only one data point was used at each concentration magnitude, then both the RMSEC and the RMSEP magnitudes would be much lower.

The residual error plot for actual vs. predicted concentrations of the calibration model was obtained. The margins of error within the figure suggested that there could be a change of the ratio of the loading of sample C to sample B than the predicted magnitude. However, since there was no observed trend within the figure, then the data was considered to be normal.

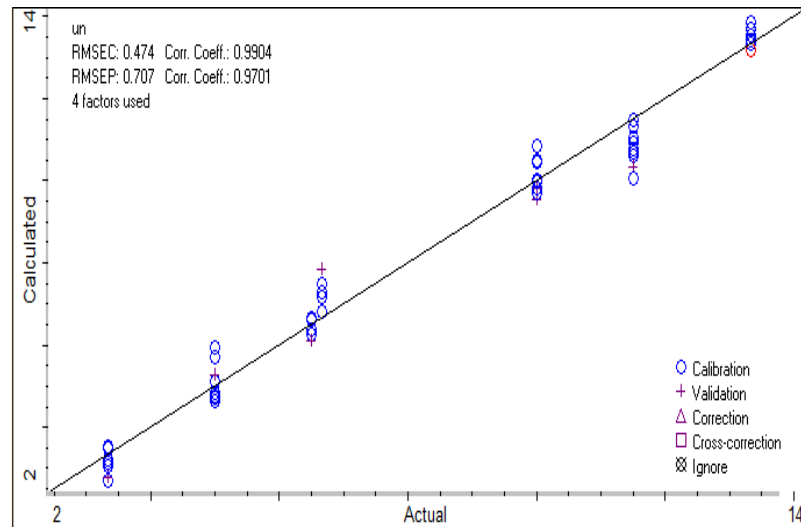


Figure 5-4: Calibration model for the concentration obtained by using the spectra analysis on the 1<sup>st</sup> overtone region to determine the ratio of the concentrations. Scales are unitless.



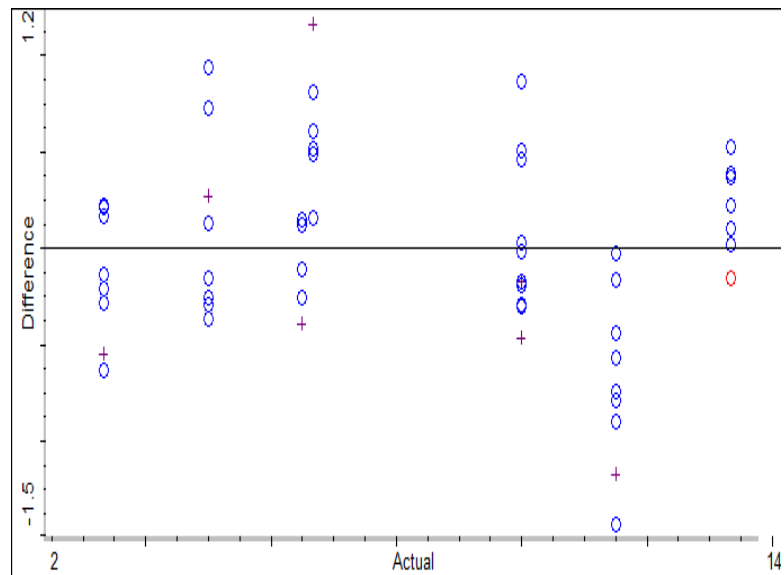


Figure 5-5: Residual error plot of actual vs. predicted concentration for the spectra analysis of the 1st overtone to determine the ratio of the concentrations. Scales are unitless.

The calibration model was obtained using four partial least square, PLS, factors. Homogeneity of the solid sample was difficult to achieve when two different samples, sample A and B, were mixed together. Hence, the absorbance of the mixed samples was not as consistent as the absorbance of the pure samples.

By fixing the concentration of samples A, B, and mixtures of A & B, it was possible to obtain a calibration model that involved these two samples. Once sample C was introduced into the mix, the calibration model changed significantly. The anti-caking agent loading concentration was changed several times until the data that corresponded to sample C was fitted on the calibration model. The ratio of sample C to B loading concentration was 141%. Sample C had 41% more of the anti-caking agent than sample B. However, it should be noted that this loading concentration of 141% was the lower bound of the ratio range that provided a linear fit. The higher end being a ratio of 153%. This suggested that a ratio

within this range, 141%-153%, would have also fitted the data on the calibration model as well.

The second experiment explored the same procedure, but with inserting the actual concentrations of 4.3 lb/ton and 2.9 lb/ton for 20053365 and 20053371 respectively. The calibration model was then developed using this data for the same sample mixtures. The calibration model, Figure 5-6, had a better fit than Figure 5-4.

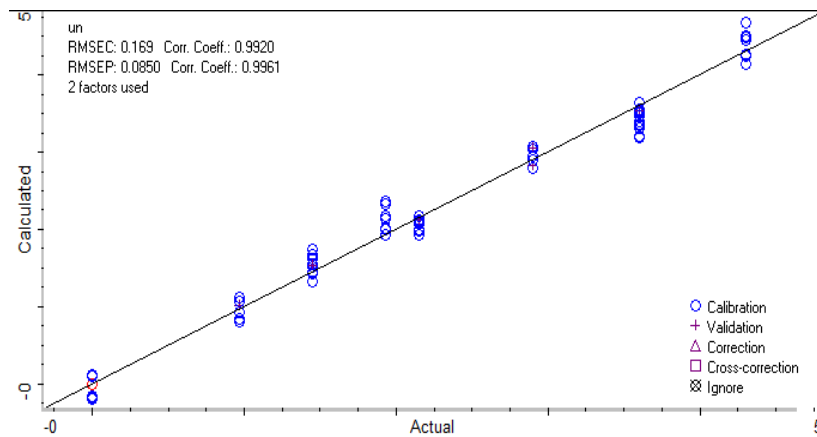


Figure 5-6: Calibration model for the concentration obtained by using the spectra analysis on the 1st overtone region given the ratio between the two samples. Scales are unitless.

The calibration model yielded a cross-validation factor, RMSEC, of 0.169 and an independent validation, RMSEP, of 0.085. The correlation coefficients of both factors, 0.9920, and 0.9961 suggested a good fit of the validation points to the calibration model. Notice that the spread of the data was smaller for each sample mixture. This provided lower magnitudes of both RMSEC and RMSEP.

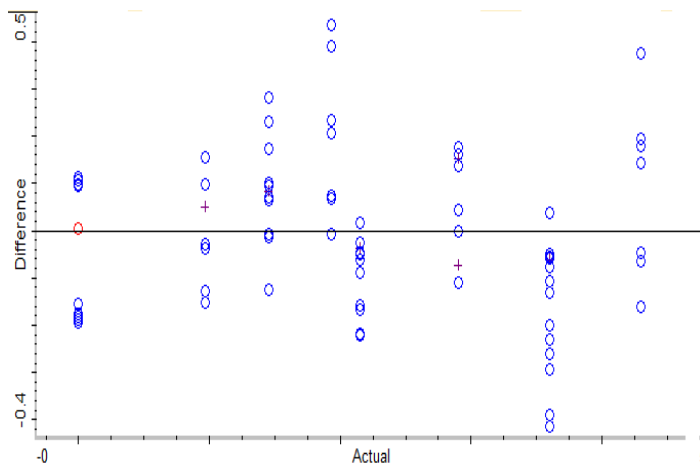


Figure 5-7: Residual error plot of actual vs. predicted concentration for the spectra analysis of the 1st overtone given the ratio between the two samples.

As seen in figure 5-7, there was no trend between the residual errors, suggesting that the data is normal. Additionally, two factors were only utilized in the second experiment, while 4 factors were utilized in the first experiment. This indicated that the provided sample concentrations delivered a better fit than the predicted ratio of 1.41. This implied that a ratio of 1.48 better fitted the data than a ratio of 1.41. The weight percent margin of errors calculated were an average of  $\pm 0.25\%$ .

#### 5.4 Conclusion

FT-NIR analyzer was utilized to determine the ratio of the concentrations of anti-caking agents loaded onto KCl. Several samples were mixed together in order to provide multiple data points for different sample concentrations. The samples were inserted into clear glass vials and put over the integrated sphere in order to measure the absorbance. The spectra were then analyzed using the TQ Analyst software. The developed calibration model demonstrated that a concentration ratio of the amine loading, lb/ton, of 141% of sample C, code 20053365, to sample B, code 20053371, was observed. The margin of error within the multiple absorbance spectra for each sample resulted in multiple applicable ratios. The

lower end of the ratio range was approximately 141%. Therefore, a second experiment was then conducted with the known concentrations, an actual ratio of 148%. The new calibration model was a better fit to the data than the one developed in the first experiment. Additionally, two factors were only used to develop the model given the concentrations whereas four factors were used for the first experiment to determine the model without the ratio being given.

## Chapter 6 Mini-fluidic Continuous Amine Monitoring

### 6.1 Introduction

Aqueous amine solutions have been neutralized with HCl as part of the reagent conditioning process to separate KCl from NaCl in flotation vessels. The amine reagent is neutralized by the addition of HCl at a specific ratio in order to activate the amine molecule. The protonated amine molecule binds to the crystal defects in the KCl compound and increases the tendency of KCl to attach to air as part of the flotation process. Batch conditioning of the amine reagent has demonstrated a lack of homogeneity of the final solution with respect to the degree of neutralization of the solution. Due to mixing irregularities, complete protonation of the amine solution ( $\text{R-NH}_2$  to  $\text{R-NH}_3^+$ ) could not be achieved due to the formation of micelle globules that served as a protection layer against the protonation process [2]. The protective layer can be broken down however by increasing the dispersion of the amine throughout the solution and not allowing the solution to settle down [21]. Therefore, conversion of batch-to-continuous conditioning of the amine solution is explored in lab settings with the aid of dispersion-inducing instruments. Homogeneity of the neutralized amine solution has been achieved after the batch-to-continuous conversion after the mixing experiment discussed in chapter one.

Determination of the amine weight percent and the amount neutralized has been done using titration-based measurements or the Baume Scale method. These two methods require many factors that affect the final measurements of the weight percent and the percent neutralized. Further, these methods may require dilutions, drying, and pre-heating of the samples that would decrease the accuracy of the final results. Moreover, these techniques are time consuming, labor intensive, and hazardous. Titration tests are inaccurate when the

weight percent must be within 0.1 wt.% error margin. Baume scales are also as accurate as the introduced factors and cannot reach less than 1.00 wt.% error margin.

The objective is to develop an accurate, fast, non-hazardous, and continuous monitoring method to determine the weight percent amine in aqueous solutions as well as the percent neutralized. The new method uses Fourier Transform Near Infrared, FT-NIR, analyzer by using fibre-optic cables to measure the absorbance. The measuring technique does not require the sample to be taken off-line, hence there is no need for any sample manipulation or introduction of factors.

## 6.2 Experimental Setup

### 6.2.1 Lab Setup

On-line mini-fluidic experiments were carried out in the setup presented in Figures 6-1 and 6-2 under lab scale settings.



Figure 6-1: Heated water vessel (left), and the flow through cell within the transmission module of the FT-NIR (right).

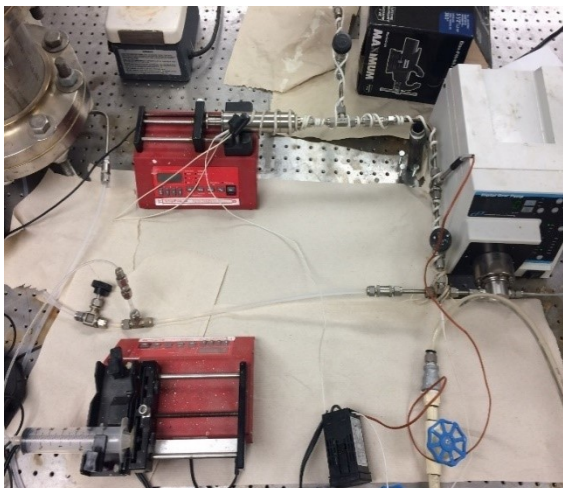


Figure 6-2: Lab setup of the inline monitoring system utilizing needle pumps for the injection of amine and HCl.

Water was stored at 50-70° C in a vessel with a built-in heater. Flow into the system was altered for each sub-experiment by utilizing a metering pump (Cole Parmer 75211-30, equipped with Micropump P23 head). The amine was initially melted and maintained at a temperature similar to that of the water, and then inserted into a syringe pump. A diluted HCl solution was also inserted into a syringe pump, and the injection rate was set to multiple flow rates depending on the desired degree of neutralization. Hot water was initially run through the PFA tubing (1/4" pre-pump, 1/8" post-pump) to pre-heat the system and prevent any solidification of amine throughout the lines. Following pre-heat, HCl was injected at an equimolar flow rate to that of the amine, adjusted to reach the desired degree of neutralization. Amine was then injected downstream of the HCl's injection port. The solution then passed through a gear pump and 3-meter length 1/8<sup>th</sup> inch diameter PFA tubing.

The HCl solution's molarity was calculated using a density meter that provided both the temperature and the density. These two properties were used in a calibration model

previously developed to obtain the weight percent of HCl present. The weight percent of HCl was then used to calculate the molarity of the solution.

### ***6.2.2 Spectrophotometry***

Since the solution was comprised of an amine molecule, the focus then was on the three overtones of the R-NH<sub>2</sub> bond. The examined wavelength number range was 10,000-4,000 cm<sup>-1</sup>. The main focus of the spectra was on the first overtone region (~5600 cm<sup>-1</sup>), the second overtone region (~6500 cm<sup>-1</sup>), and the third overtone region (~9000 cm<sup>-1</sup>). Furthermore, the absorbance region in the range of 4000 cm<sup>-1</sup> - 4500 cm<sup>-1</sup> was thoroughly examined because of the presence of a distinguishable trend in the spectra. For each experimental set, samples were collected and analyzed using commercially accepted methods to determine the amine weight percent as well as the neutralization percentage using both diluted HCl and KOH solutions. These measurements were used and referred to as the actual amine weight percent and the actual degree of neutralization.

The water flow rate was held constant throughout the experiment, but the amine and the HCl flow rates were adjusted to provide a wide range of data. The amine weight percent was in the range of 0 wt% - 3 wt%, while the HCl-to-Amine ratio was in the range of 0% - 120% for each amine weight percent.

## **6.3 Results and Discussion**

The results of this chapter were divided into two main sections; a developed regression model, and a calibration model provided by the FT-NIR software through analyzing the data. The regression model will be studied first, and then compared against the analyzer



model. The regression model includes the slope models, the single point ratio models, and the double-point normalization model as well.

### 6.3.1 Slope models

After calibration of the pump was done, homogenous mixing of the solution was achieved by changing the flow rate of the pump and keeping the overall flowrate constant at that magnitude. The absorbance results demonstrated a trend in the range of  $4000\text{ cm}^{-1}$  to  $4500\text{ cm}^{-1}$  as the HCl concentration was adjusted. The raw spectra with no smoothing applied is seen in Figure 6-3 below.

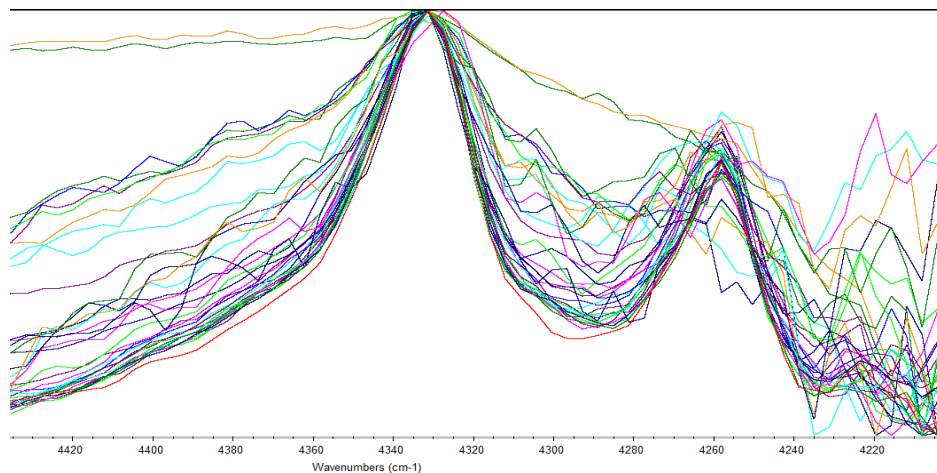


Figure 6-3: Raw absorbance spectra using the OMNIC software across the wavenumber region ( $4400 - 4258\text{ cm}^{-1}$ ).

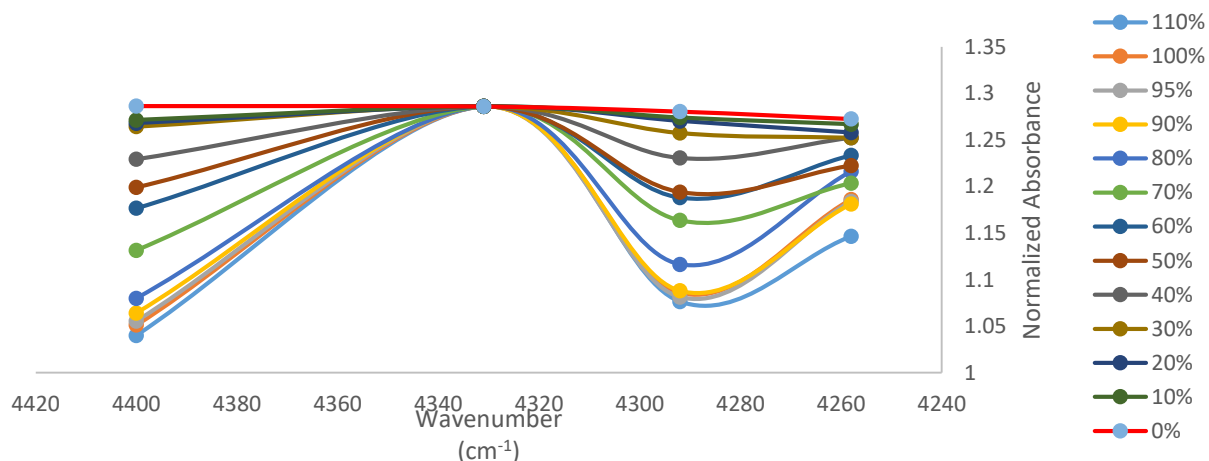


Figure 6-4: A sample of the absorbance spectra against the examined region, 4400 – 4258  $\text{cm}^{-1}$ .

Figure 6-4 illustrated the absorbance spectra within that range as a function of the HCl concentration. The wavenumber of the amine bond did not reside within this region. This trend in the absorbance spectra was due to the impact of the neutralization of the amine molecule on the carbon-carbon, C-C, bonds. Knowledge about the amine absorbance spectra, when neutralized, suggested stretching of the C-C bond taking place. This stretching of the bonds led to an increase in the absorbance specifically at 4258  $\text{cm}^{-1}$  and 4331  $\text{cm}^{-1}$ . This stretching can be accounted for by the increase in the polarity of the amine functional group,  $\text{R-NH}_2$  to  $\text{R-NH}_3^+$ . The transfer of the electron lone pair of the nitrogen atom to a covalent bond forming with a hydrogen atom resulted in a decrease in the overall electronegativity, EN, of the functional group. This decrease in the EN allowed the C-C bonds to stretch away from the functional group, that led to an increase in the absorbance as the amine molecule was neutralized. Appendix A examined the amine overtone regions and compared their results with the 4400-4250  $\text{cm}^{-1}$  region.

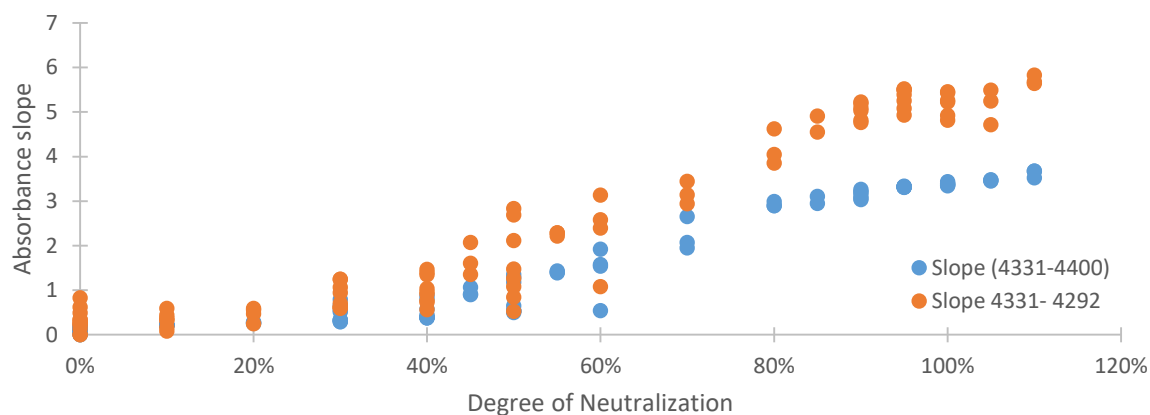


Figure 6-5: Normalized absorbance data for two slope regions vs. DoN.

Using the spectra data provided in Figure 6-3, the slope can be calculated between either the regions  $4400\text{ cm}^{-1}$  and  $4330\text{ cm}^{-1}$ , or between  $4330\text{ cm}^{-1}$  and  $4292\text{ cm}^{-1}$ . As seen in the above figure, the magnitude of the slope started to remain constant within a 10% margin after reaching 90% degree of neutralization, (DoN). This indicated that the solution was becoming homogeneously neutralized as the unreacted amine molecules became scarce in the solution. Furthermore, minimal slope differences, less than 1%, was observed between 100% and 110% DoN. This demonstrated that the wavenumber range that was chosen was only affected by the neutralization reaction and not by the presence of HCl. The slopes were then used to develop two models to predict the neutralization degree of the solution. The data that were chosen belonged to amine weight percentages 1.0%, 2.0%, 2.5%, and 3.0%. Regardless of the amine weight percent, the DON was calculated within a maximum margin of error magnitudes of 20% DoN.

The two slope models managed to predict the degree of neutralization without relying on the weight percent. However, a margin of error of 20% DoN was considerably higher than

the required minimum accuracy of error margins, +/- 8% DoN. Hence, a single point area ratio model was examined to determine its viability in determining the DoN.

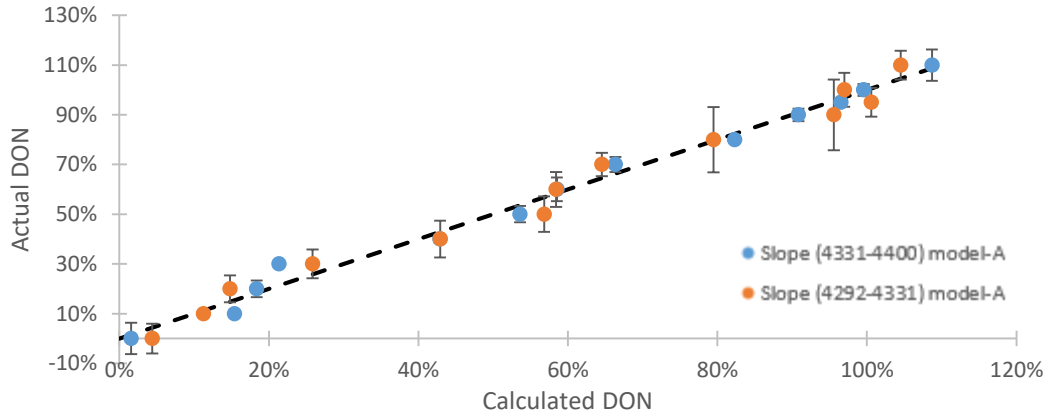


Figure 6-6: Actual DoN vs. Calculated DoN for slope models developed after applying single-point normalization at 4331  $\text{cm}^{-1}$ .

### 6.3.2 Single-point ratio models

The ratio model was developed by normalizing all of the absorbance points to the reference wavenumber 4331  $\text{cm}^{-1}$  that represented an absorbance value of one as seen in figure 6-7 below.

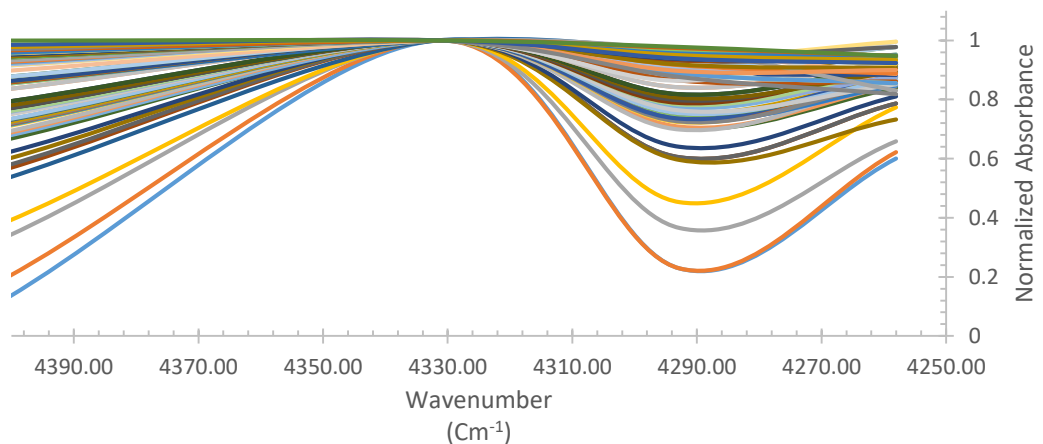


Figure 6-7: Single-point normalization of the absorbance spectra at 4331  $\text{cm}^{-1}$  vs. wavenumber.

Absorbance spectra that corresponded to 0% degree of neutralization had magnitudes of one across in Figure 6-7. As the degree of neutralization increased above 0%, normalized absorbance at certain wavenumbers, 4400  $\text{cm}^{-1}$  and 4291  $\text{cm}^{-1}$ , started to decrease below a value of one. Gauss quadrature theorem was utilized to calculate the area under the curve and correlate it to the degree of neutralization. A model was then developed using the area to predict the degree of neutralization. The figure below demonstrated the actual against the calculated degree of neutralization using the area under the curve model.

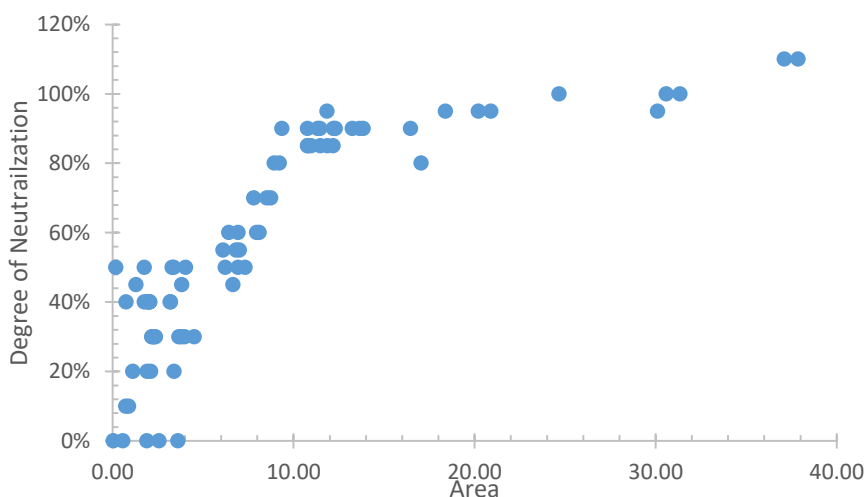


Figure 6-8: DoN vs area under the curve for points (4331-4258  $\text{cm}^{-1}$ ) after applying single-point normalization on the absorbance spectra.

The single-point normalization figure above demonstrated inconsistencies of the area magnitudes as the degree of neutralization increased. These inconsistencies and outliers, from 0% to 80% and from 80% to 110%, could be the result of the change of the amine weight percent. Using a single-point normalization model implied that the weight percent of amine did not affect the absorbance spectra. This assumption was the reason behind the figure above not following a diagonal line.

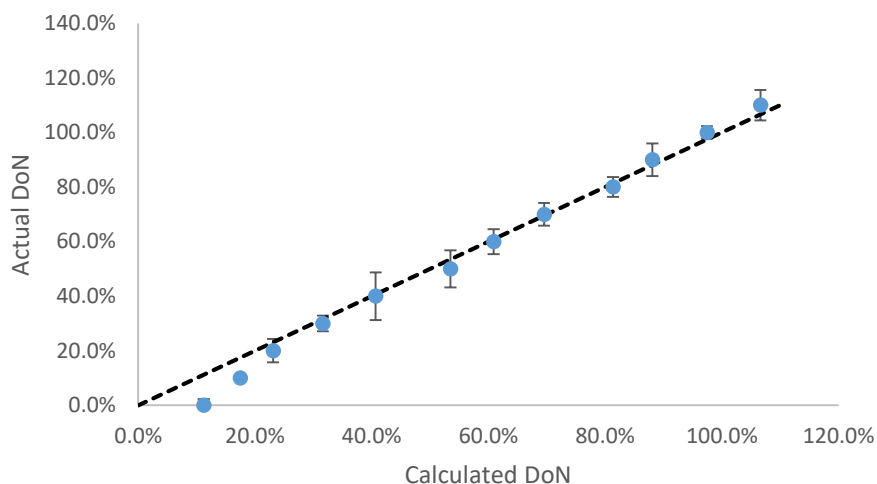


Figure 6-9: Actual vs. Calculated DoN using the single-point normalization and area model with 95% C.I.

Regardless however, if a single-point normalization model was developed by utilizing multiple functions to predict the degree of neutralization, the model would prove accurate. However, the inconsistencies within the results from using a single-point normalization model would make the model susceptible to instantaneous data point changes such as at the 80% DoN sudden change. The model was accurate within 95% confidence intervals above 20% degree of neutralization. A maximum margin of error of 20% DoN was achieved through the single-point area ratio model. This margin of error was higher than the minimum margin. The degree of neutralization was examined for each amine weight percent separately.

In order to overcome the inconsistencies observed in the previous model, the data points were divided into three separate categories; 1 wt%, 2 wt%, and 3wt%. this division nullified the reliance on the weight percent and its contribution to the spectra, and put more emphasis on the degree of neutralization. Figure 6-10 represented the relationship observed between the degree of neutralization and the normalized absorbance spectra at  $4400\text{ cm}^{-1}$ .

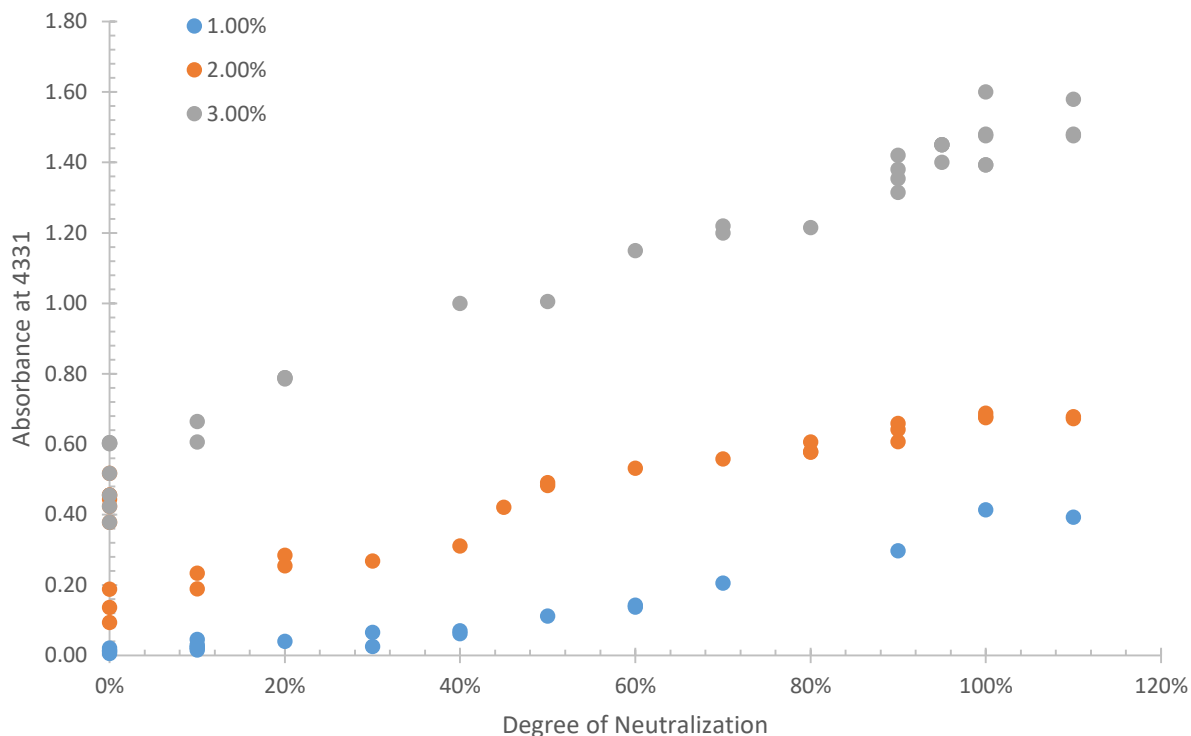


Figure 6-10: Absorbance for 1%, 2%, and 3% weight percent vs. the DoN at  $4331\text{ cm}^{-1}$ .

The slope of the data changed across different amine weight percent concentrations. This suggested a certain degree of reliance on the weight percent that did in fact introduce errors in the single-point normalization model presented earlier when all the data points were put together. Using the relationship between the degree of neutralization and the absorbance, a function that was reliant on the area changes in the absorbance due to the addition of HCl was used to predict the degree of neutralization. The predicted values were then plotted against the actual values of the degree of neutralization. Figure 6-11 demonstrated how well the functions predicted the degree of neutralization for the three weight percent values. These plots were obtained without using any filters or application of any normalization standards. The area under the curve was calculated for each raw spectrum, and the degree of absorbance was plotted against it. This model concluded that both the degree of

neutralization and the weight percent did in fact impact the absorbance. The respective margins of errors for 1 wt%, 2 wt%, and 3 wt% were 8.5% DoN, 13% DoN, and 7.5% DoN respectively.

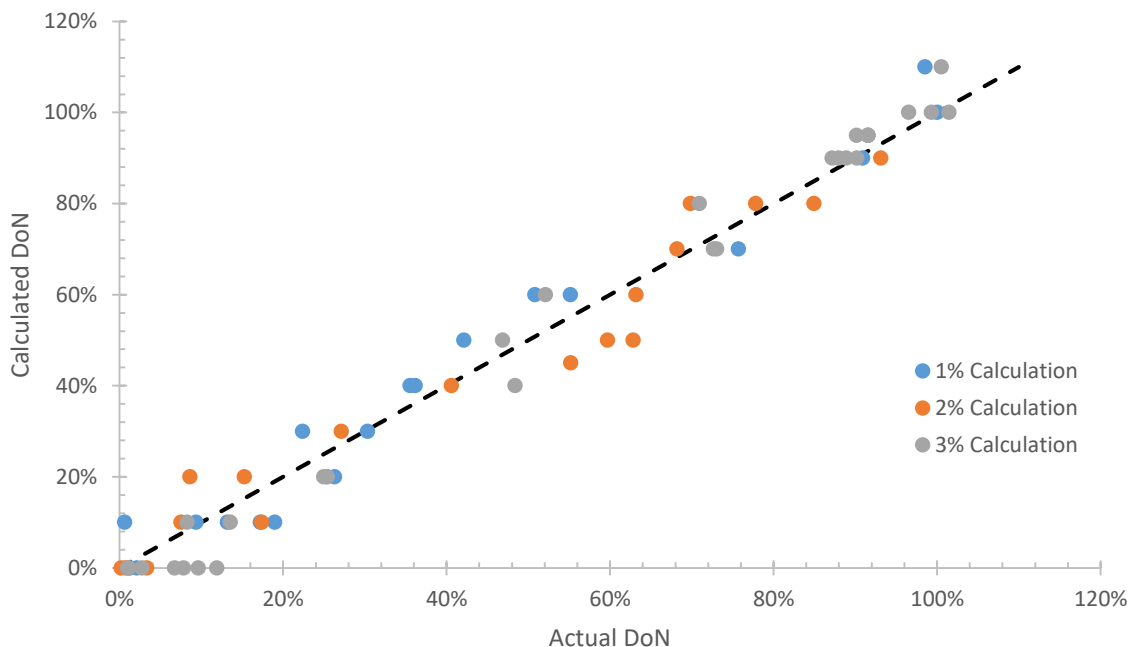


Figure 6-11: Calculated vs. actual DoN using single-point normalization at 4331  $\text{cm}^{-1}$ . Data was divided to three separate figures to nullify the effect of weight percent on the absorbance.

### 6.3.3 Two-Point normalization model

Due to the inadequacy of using a single-point normalization to determine both the degree of neutralization and the weight percent, double-point normalization was applied on the raw spectra with the two points being 4331  $\text{cm}^{-1}$  and 4258  $\text{cm}^{-1}$ . Figure 6-12 represents the double-point normalization applied for 1 wt%, 2 wt%, and 3 wt%.



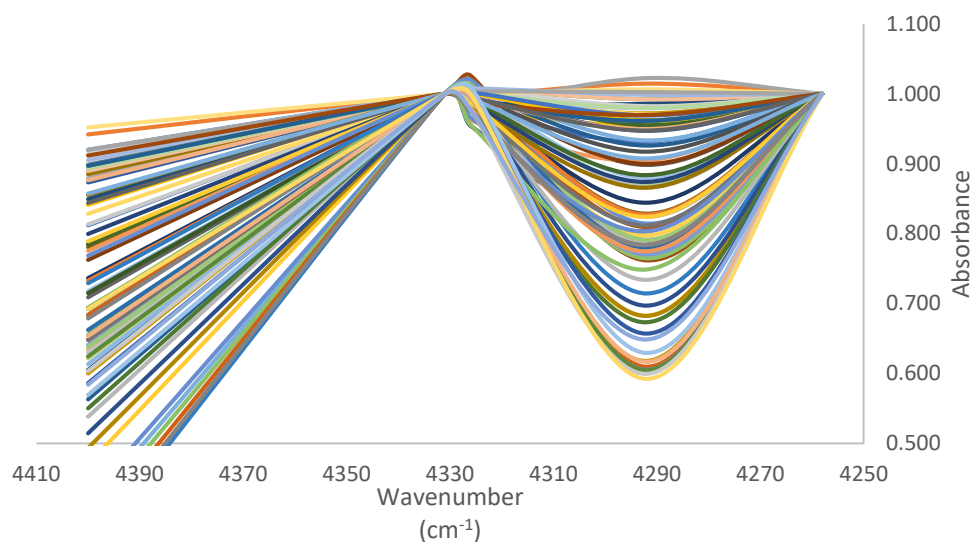


Figure 6-12: Two-point normalization at  $4331\text{ cm}^{-1}$  &  $4258\text{ cm}^{-1}$  of the raw spectra. Using the slope between  $4400\text{ cm}^{-1}$  and  $4331\text{ cm}^{-1}$ , a calibration curve was developed that related the slope between the mentioned data points and the degree of neutralization. The only region considered for calibration was between 0% and 100% degree of neutralization. Greater neutralization percentages were used as validation points to determine the accuracy of the calibration model. The following figure represented the relationship between the slope and the degree of neutralization after implementing a two-point normalization, commonly known as a line normalization.

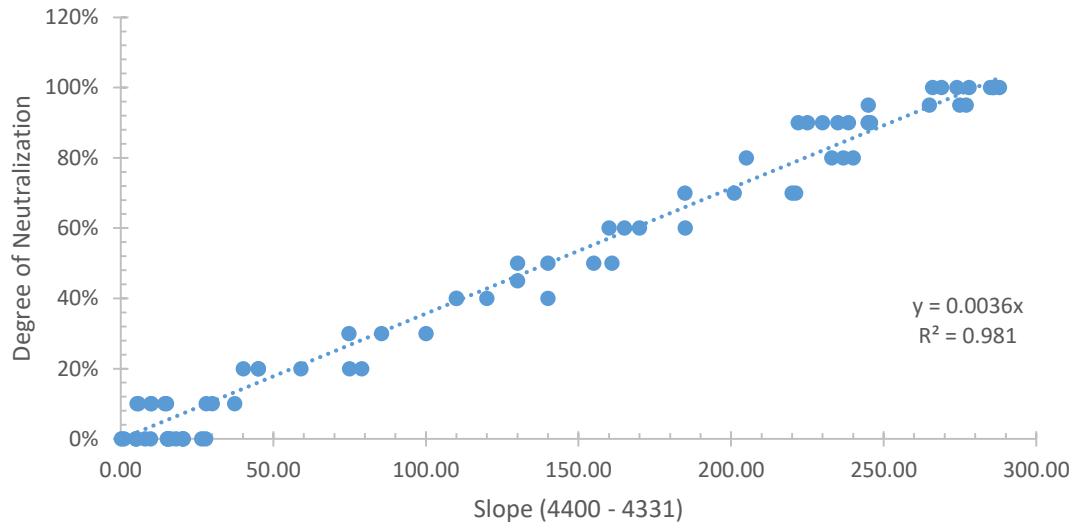


Figure 6-13: DoN vs. slope (4400-4331  $\text{cm}^{-1}$ ) for two-point normalization model. Using this model, a predicted vs. actual degree of neutralization diagram was obtained to determine the accuracy of the double-point normalization model.

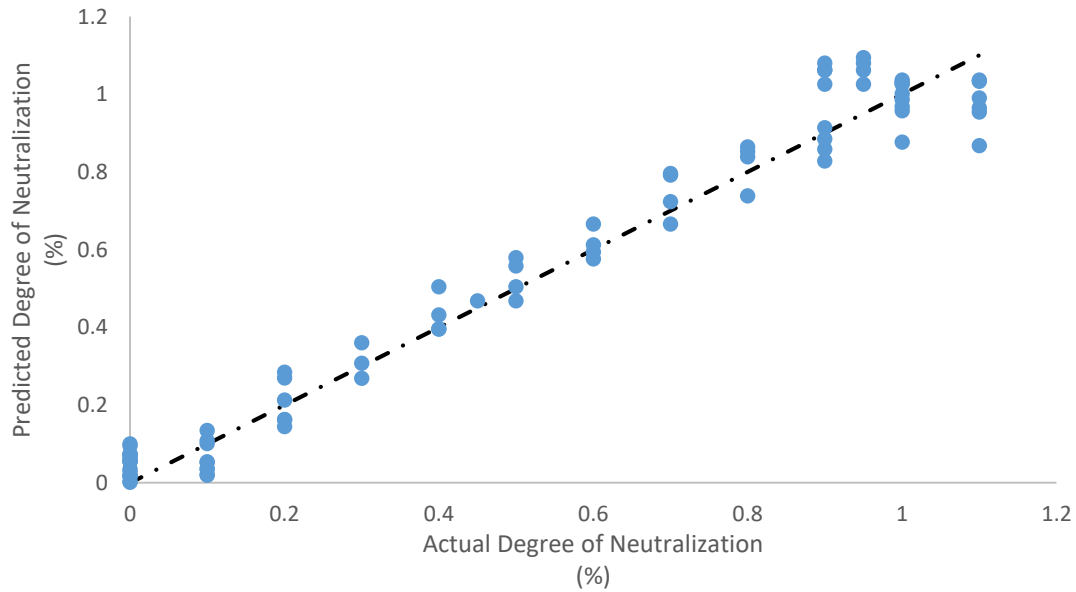


Figure 6-14: Predicted DoN Vs. Actual DoN using the two-point normalization model.

As seen in Figure 6-13 and 6-14, the model predicted the degree of neutralization accurately with a standard error magnitude of 4%, while also maintaining the physical limit of 100% DoN even when excess HCl was added.

The next step was to determine the amine weight percent using the degree of neutralization along with other features of the data. A regression model was developed from absorption data at 4331  $\text{cm}^{-1}$  (Figure 6-10) to determine the amine weight percent using the degree of neutralization, resulting in the predictions illustrated in Figure 6-15.

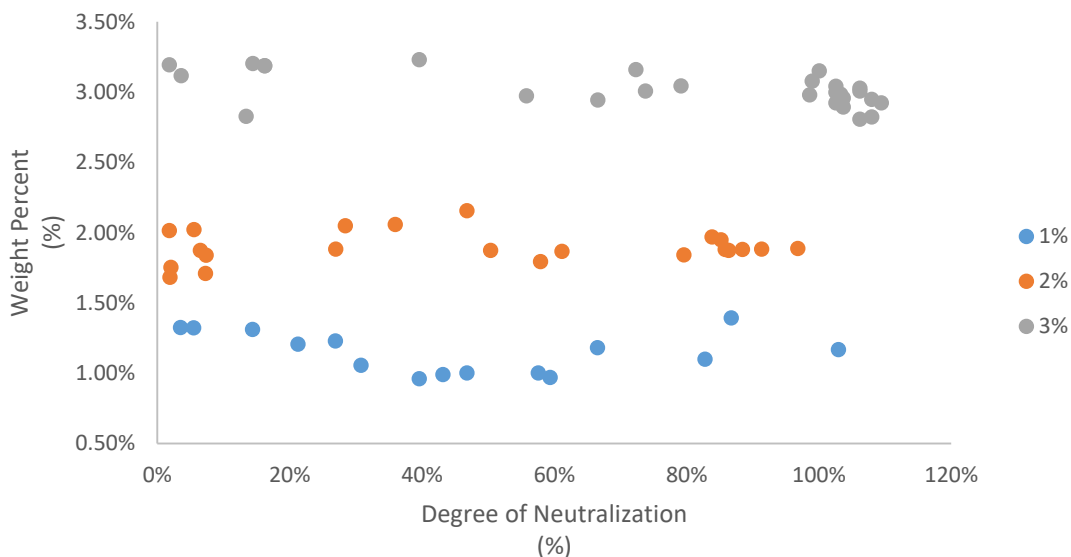


Figure 6-15: Weight percent vs. DoN using a numerical model for 1 wt%, 2 wt%, and 3 wt%.

#### 6.3.4 *Antaris II TQ-Analyst Results*

All of the examined models were compared against a reference model that was developed using the TQ Analyst software. A 1 mm path length quartz cuvette was utilized in the flow-through transmission cell of the FT-NIR instrument in order to measure the absorbance. The transmission heated cell was kept at a temperature that was equivalent to the solutions. A background sample of heated water was initially taken to ensure that any environmental

changes within the lab were accounted for in the sample spectra. 50 samples were taken in for each weight percent, with 5-10 validation points utilized for each. 10 scans were collected for each sample with a resolution of  $4\text{ cm}^{-1}$  in 5 seconds. A partial least square analysis, PLS, was utilized for the basis of absorbance calibration on the wavenumber region chosen for the analysis,  $4400\text{-}4250\text{ cm}^{-1}$ .

Using filters to reduce the noise in the spectra, the model for the three different amine weight percent managed to predict the degree of neutralization of amine with a root mean square error of calibration of 7.17% and a root mean square error of prediction of 6.33%. The correlation coefficients were 96.6% and 99.0% respectively. In comparison with the two-point normalization regression model previously mentioned, the correlation coefficient was 97.5%. The two-point normalization model used managed to predict both the degree of neutralization and the weight percent with margins of errors of 4% DoN and 0.2 wt% respectively, while the software model had margins of errors of 6% DoN and 0.065 wt%. The following two figures, figure 6-16 and 6-17 represented the calibrated Antaris model for the DoN and its residual error difference.

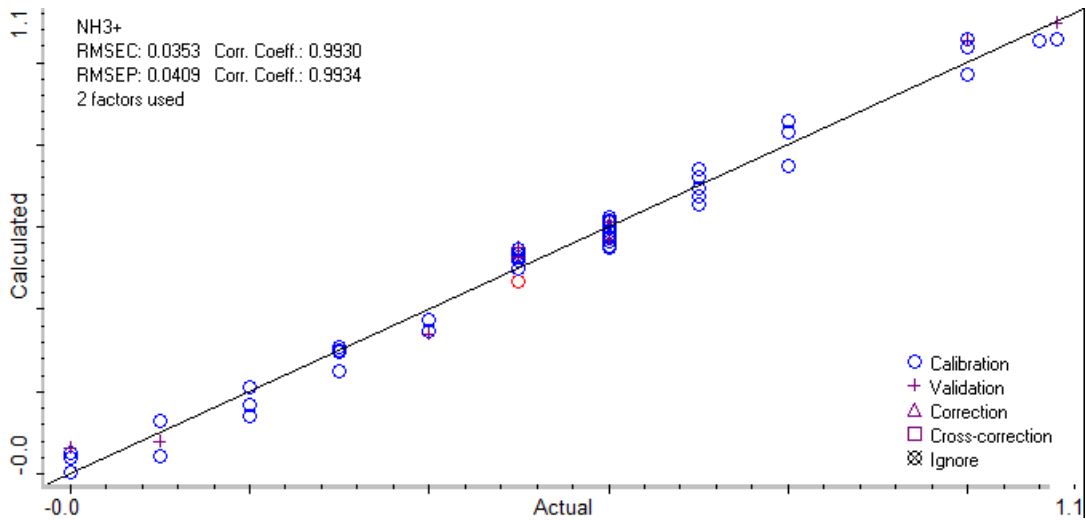


Figure 6-16: Calculated vs. actual DoN for 1wt%, 2wt%, and 3 wt% using Antaris software.

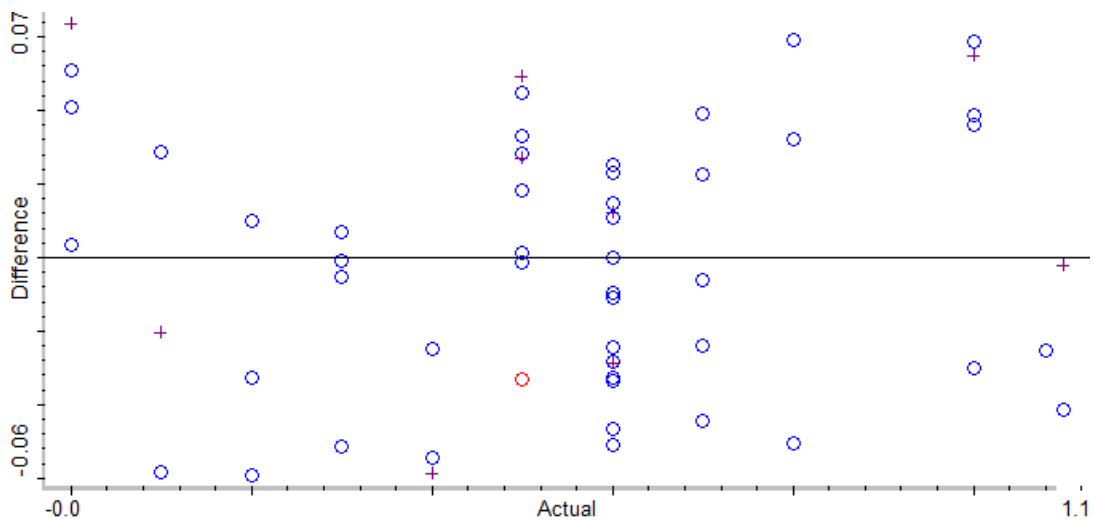


Figure 6-17: Residual error difference of the DoN data at 1%, 2%, and 3%.

The weight percent calibrated model through the software provided better results than the regression model. As seen in figures 6-18 and 6-19, a margin of error of 0.06 wt% was achieved. This margin of error was smaller than the one achieved through using the regression model, 0.15 wt%.

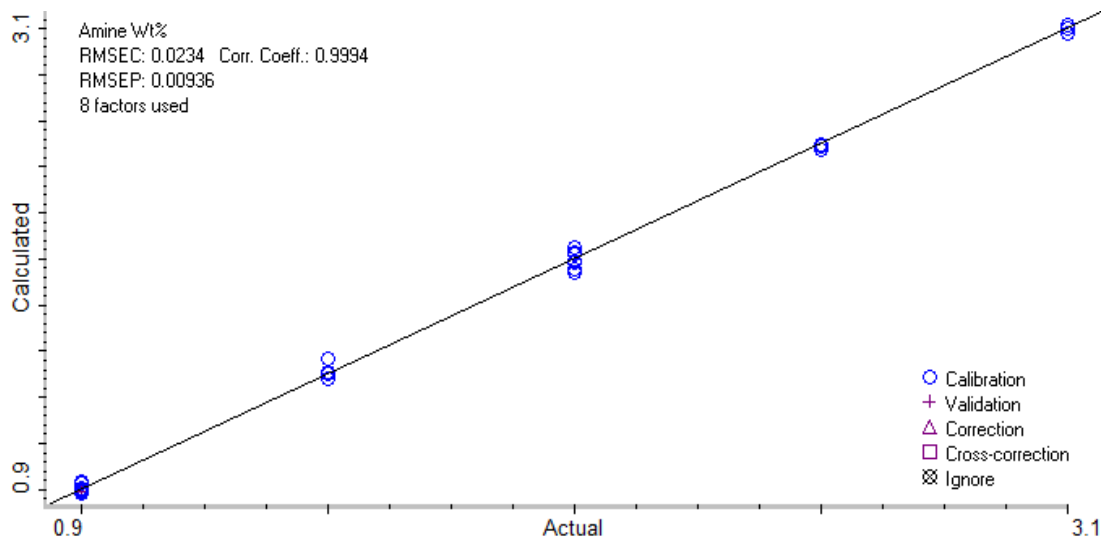


Figure 6-18: Calculated vs. Actual weight percent using the Antaris software

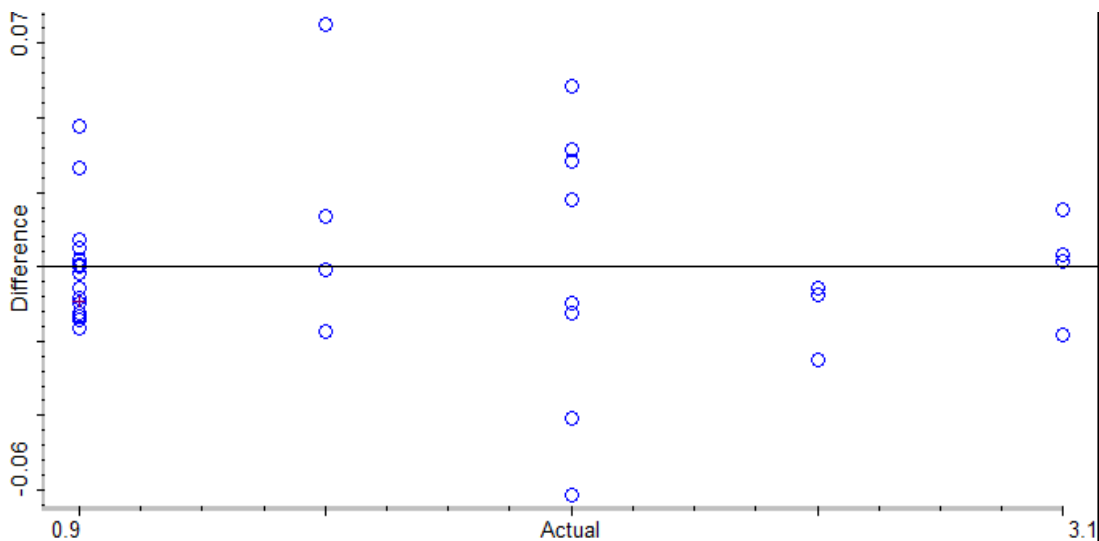


Figure 6-19: Residual error plot for the amine weight percent calibrated model using the Antaris software

## 6.4 Conclusion

The Antaris II FT-NIR analyzer was utilized to develop multiple models to predict both the degree of neutralization and the amine weight percent as part of the reagent conditioning process in flotation applications. The absorbance was measured using a built-in heated transmission module with a flow-through cell equipped. The results demonstrated

multiple applicable models that could be used to calculate the degree of neutralization from the wavenumber region of  $4400\text{ cm}^{-1}$  to  $4250\text{ cm}^{-1}$ .

## Chapter 7 Conclusion

This thesis has presented the results of mixing studies relevant to the selection of appropriate static mixing elements in batch-to-continuous conversion of amine reagent preparation for potash processing, as well a summary of the successful application of FT-NIR as a spectroscopy-based monitoring method of amine dosing and degree of neutralization within loadout and flotation reagent preparation units. Based on the results presented, the following recommendations were made to Mosaic as a result of this work:

- 1) During batch-to-continuous retrofit applications, installation of an orifice plate directly downstream of amine injection is recommended to promote rapid dispersion of the amine, with a preferred process line size of 1" to promote continued dispersion. If a commercial static mixing device is selected, a minimum of 6 elements is required to achieve +85% dispersion.
- 2) FT-NIR was able to successfully monitor amine dosing in oil for anti-caking applications through analysis of the first derivative of the second and third overtone regions ( $6700$  and  $9700\text{ cm}^{-1}$ ). With temperature correction, weight percent's ranging from 0 to 7 wt% were successfully quantified to within  $\pm 0.1$  wt%.
- 3) Anti-caking addition to solid granular product was accurately quantified for loadings from 0 to 5 lb/ton to within  $\pm 0.3$  lb/ton. These measurements were determined from un-processed granular products as homogenous and heterogeneous samples using the integrating sphere module, but not for crushed samples.
- 4) Analysis of the spectral response for wave numbers in the range of  $4250\text{ cm}^{-1}$  –  $4400\text{ cm}^{-1}$  yields amine weight percent and degree of neutralization measurements



accurate to within 0.04 wt%, and 6% DoN. A reduced resolution model is proposed which would enable accurate measurements of amine weight percent and degree of neutralization from absorbance data at 4400, 4331 and 4258  $\text{cm}^{-1}$ . The reduced resolution model may prove useful for porting this methodology between instruments, where proprietary software platforms do not always enable direct import/export of developed calibration models.

## References

- [1] Burdukova, E., & Laskowski, J. (2009). Effect of insoluble amine on bubble surfaces on particle–bubble attachment in potash flotation. *Canadian Journal of Chemical Engineering*, **87**(3), 441-447.
- [2] Yoshioka, T., Ikeuchi, K., Hashida, M., Muranishi, S., & Sezaki, H. (1982). Prolonged release of bleomycin from parenteral gelatin sphere-in-oil-in-water multiple emulsion. *Chemical & Pharmaceutical Bulletin*, **30**(4), 1408-15.
- [3] Kachko, Van Der Ham, Bardow, Vlugt, & Goetheer. (2016). Comparison of Raman, NIR, and ATR FTIR spectroscopy as analytical tools for in-line monitoring of CO<sub>2</sub> concentration in an amine gas treating process. *International Journal of Greenhouse Gas Control*, **47**, 17-24.
- [4] Mukhopadhyay, Banerjee, Koll, Filarowski, & Mukherjee. (2006). Ground and excited state proton transfer reaction of salicylidine-3,4,7-methyl amine in micelles. *Chemical Physics Letters*, **420**(4), 316-320.
- [5] Malmstrøm, J. (2012). Characterization of 40 kDa poly(ethylene glycol) polymers by proton transfer reaction QTOF mass spectrometry and 1 H-NMR spectroscopy. *Analytical and Bioanalytical Chemistry*, **403**(4), 1167-1177.
- [6] Bate, & Burns. (2010). Effect of total organic carbon content and structure on the electrokinetic behavior of organoclay suspensions. *Journal of Colloid And Interface Science*, **343**(1), 58-64.
- [7] Grassi, Amigo, Lyndgaard, Foschino, & Casiraghi. (2014). Beer fermentation: Monitoring of process parameters by FT-NIR and multivariate data analysis. *Food Chemistry*, **155**, 279-286.
- [8] Niu, Zhao, Jia, & Li. (2012). A feasibility study on quantitative analysis of glucose and fructose in lotus root powder by FT-NIR spectroscopy and chemometrics. *Food Chemistry*, **133**(2), 592-597.
- [9] Xu, Yan, Cai, & Yu. (2013). Untargeted detection and quantitative analysis of poplar balata (PB) in Chinese propolis by FT-NIR spectroscopy and chemometrics. *Food Chemistry*, **141**(4), 4132-4137.
- [10] Jiang, H., Liu, G., Mei, C., & Chen, Q. (2013). Qualitative and quantitative analysis in solid-state fermentation of protein feed by FT-NIR spectroscopy integrated with multivariate data analysis. *Analytical Methods*, **5**(7), 1872-1880.

- [11] Unger, Ozaki, Pfeifer, & Siesler. (2014). 2DCOS and PCMW2D analyses of FT-IR/ATR and FT-NIR spectra monitoring the deuterium/hydrogen exchange in liquid D<sub>2</sub>O. *Journal of Molecular Structure, Journal of Molecular Structure*.
- [12] Gabriela Budinova, Ivor Dominak, & Todd Strother. (2007). Polymerization Cure Rates using FT-NIR Spectroscopy. *Thermo Fisher Scientific Inc*.
- [13] Pineda, A., et al. (2012). "Preliminary evaluation of biogenic amines content in Chilean young varietal wines by HPLC." *Food Control* **23**(1): 251-257.
- [14] De Beer, T., et al. (2011). "Near infrared and Raman spectroscopy for the in-process monitoring of pharmaceutical production processes." *International Journal of Pharmaceutics* **417**(1-2): 32-47.
- [15] Abd El-Ghaffar, M. A., et al. (2010). "Synthesis of glycidyl methacrylate containing diethanol amine and its binary copolymers with ethyl methacrylate and butyl methacrylate as nano-size chelating resins for removal of heavy metal ions." *Journal of Applied Polymer Science* **115**(5): 3063-3073.
- [16] Yalamanchili, & Miller. (1995). Removal of insoluble slimes from potash ore by air-sparged hydrocyclone flotation. *Minerals Engineering*, **8**(1), 169-177.
- [17] Perucca, C. F. (2003). Potash processing in Saskatchewan - A review of process technologies. *CIM Bulletin*, **96**(1070), 61-65.
- [18] Imae, T., & Ikeda, S. (1985). Formation of rodlike micelles of dimethyloleylamine oxide in aqueous solutions: Effects of addition of HCl and NaCl on the micelle size and the intermicellar interaction. *Colloid and Polymer Science*, **263**(9), 756-766.
- [19] Yoshioka, T., Ikeuchi, K., Hashida, M., Muranishi, S., & Sezaki, H. (1982). Prolonged release of bleomycin from parenteral gelatin sphere-in-oil-in-water multiple emulsion. *Chemical & Pharmaceutical Bulletin*, **30**(4), 1408-15.
- [20] Fukushima, S., Juni, K., & Nakano, M. (1983). Preparation of and drug release from W/O/W type double emulsions containing anticancer agents. *Chemical & Pharmaceutical Bulletin*, **31**(11), 4048-56.
- [21] Silva-Cunha, A., Grossiord, J.L., Puisieux, F., & Seiller, M. (1997). W/O/W multiple emulsions of insulin containing a protease inhibitor and an absorption enhancer: Preparation, characterization and determination of stability towards proteases in vitro. *International Journal of Pharmaceutics*, **158**(1), 79-89.

- [22] A. Silva Cunha, J.L. Grossiord, M. Seiller, Pharmaceutical applications, in: J.L. Grossiord, M. Seiller (1996) Multiple Emulsions: Structure, Properties, and Applications, Editions de Sante, Paris, pp. 279-312.
- [23] Tedajo, G.M, Seiller, M, Prognon, P, & Grossiord, J.L. (2001). PH compartmented w/o/w multiple emulsion: A diffusion study. *Journal of Controlled Release*, **75**(1), 45-53.
- [24] Foot, D., Huiatt, J. L, Froisland, L. J, & Kramer, Deborah A. (1984). *Potash recovery from process and waste brines by solar evaporation and flotation*. U.S. Dept. of the Interior, Bureau of Mines.
- [25] Hammoudi, M., Legrand, J., Si-Ahmed, E.K., & Salem, A. (2008). Flow analysis by pulsed ultrasonic velocimetry technique in Sulzer SMX static mixer. *Chemical Engineering Journal*, **139**(3), 562-574.
- [26] Theron, F., & Sauze, N. Le. (2011). Comparison between three static mixers for emulsification in turbulent flow. *International Journal of Multiphase Flow*, **37**(5), 488-500.
- [27] Jaffer, S., & Wood, P. (1998). Quantification of laminar mixing in the kenics static mixer: An experimental study. *Canadian Journal of Chemical Engineering*, **76**(3), 516-521.
- [28] Hammoudi, M., Legrand, J., Si-Ahmed, E.K., & Salem, A. (2008). Flow analysis by pulsed ultrasonic velocimetry technique in Sulzer SMX static mixer. *Chemical Engineering Journal*, **139**(3), 562-574.
- [29] Regner, Mårten, Östergren, Karin, & Trägårdh, Christian. (2006). Effects of geometry and flow rate on secondary flow and the mixing process in static mixers—a numerical study. *Chemical Engineering Science*, **61**(18), 6133-6141.
- [30] Matsuyama, Kazuo, Mine, Koji, Kubo, Hideaki, Aoki, Nobuaki, & Mae, Kazuhiro. (2010). Optimization methodology of operation of orifice-shaped micromixer based on micro-jet concept. *Chemical Engineering Science*, **65**(22), 5912-5920.
- [31] Falk, L., & Commenge, J.-M. (2010). Performance comparison of micromixers. *Chemical Engineering Science*, **65**(1), 405-411.
- [32] Angle, & Hamza. (2006). Predicting the sizes of toluene-diluted heavy oil emulsions in turbulent flow Part 2: Hinze–Kolmogorov based model adapted for increased oil fractions and energy dissipation in a stirred tank. *Chemical Engineering Science*, **61**(22), 7325-7335.

- [33] Mukherjee, Wrenn, & Ramachandran. (2012). Relationship between size of oil droplet generated during chemical dispersion of crude oil and energy dissipation rate: Dimensionless, scaling, and experimental analysis. *Chemical Engineering Science*, **68**(1), 432-442.

## Appendix A

As stated in chapters four and five, the three overtones of the amine bond were utilized to calculate the amine weight percent whereas in chapter six, the carbon-carbon region of 4400-4250  $\text{cm}^{-1}$  was utilized instead. The amine overtones were initially examined to determine the amine weight percent in the aqueous neutralized solution prior to the use of the C-C bond region. Due to the overlapping of the water bond's overtones with the amine bond's overtones, the absorbance within these regions could not be accounted for either bond. Water was then added to the background reference spectrum in order to negate its absorbance from the experimental data and to only observe the amine's bond absorbance. Figures 0-1, 0-2, and 0-3 represent the three overtones of the amine bond while water was part of the background reference spectrum.

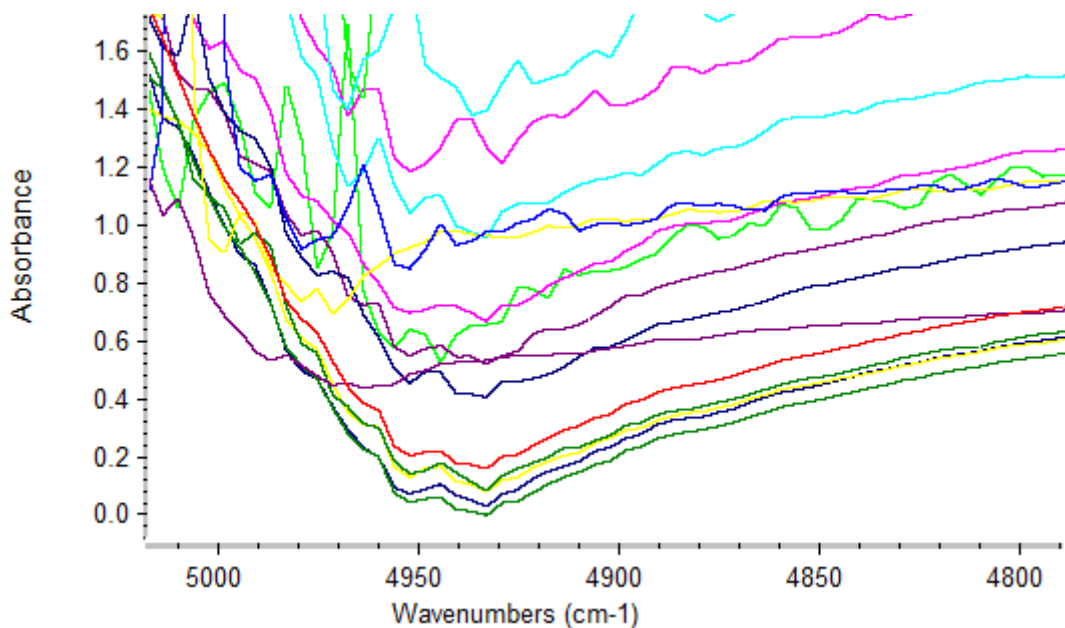


Figure 0-1: 1<sup>st</sup> overtone region of amine bond during the amine neutralization process.

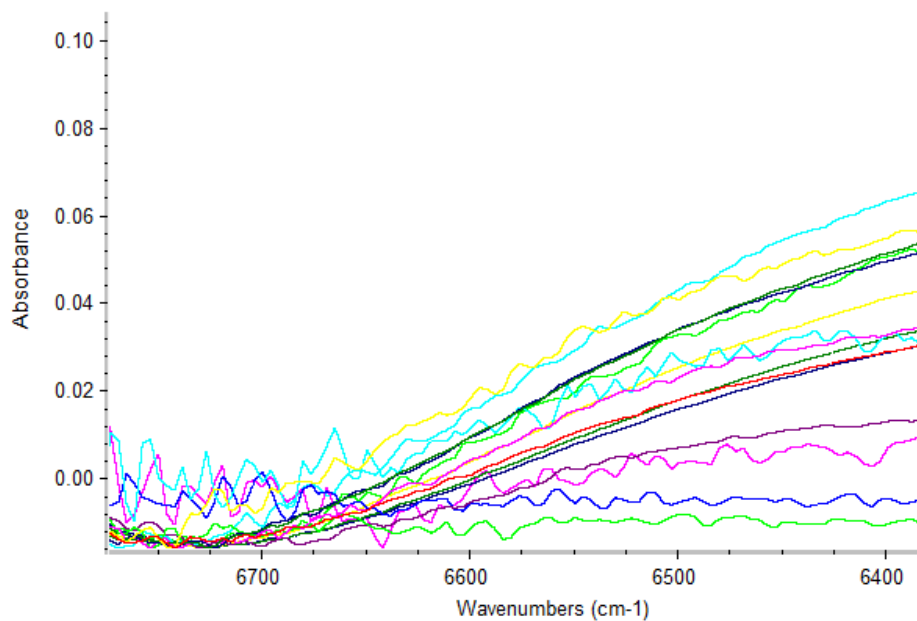


Figure 0-2: 2<sup>nd</sup> overtone region of amine bond during the amine neutralization process.

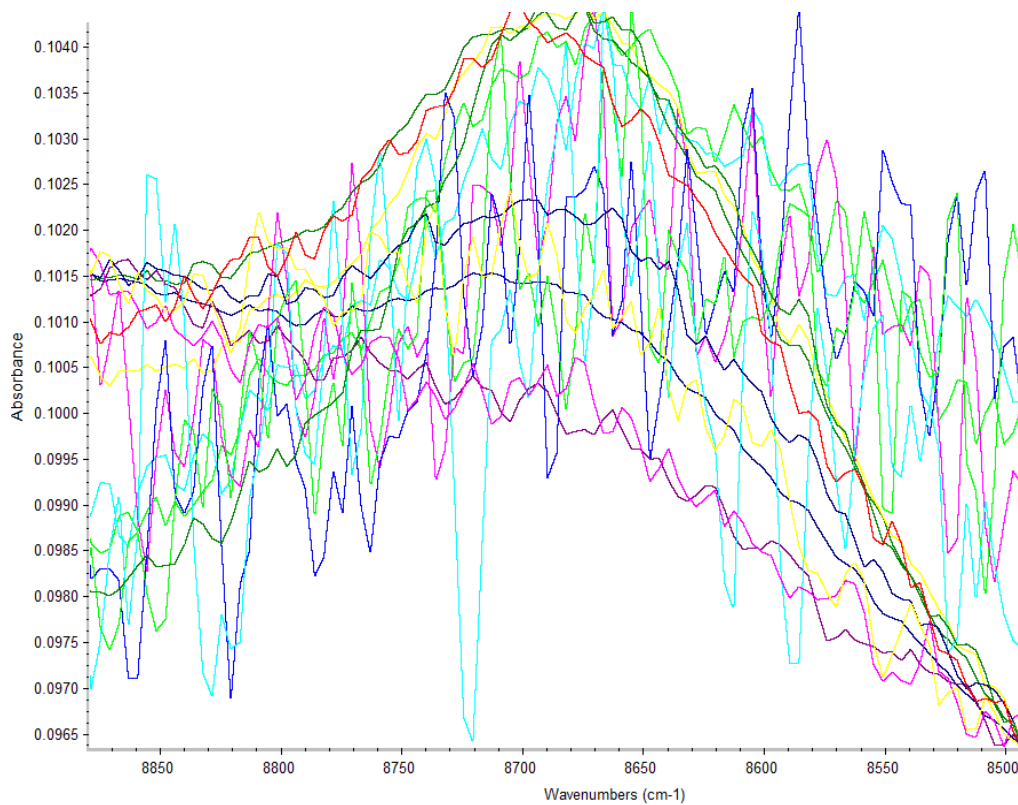


Figure 0-3: 3<sup>rd</sup> overtone region of amine bond during the amine neutralization process.

These three overtones were utilized separately and together in order to obtain a best-fit model using the Antaris software, and by also applying smoothing filters to decrease the

amount of noise. In the first overtone, a shift in the absorbance minimum peak was observed from  $4970\text{ cm}^{-1}$  to  $4940\text{ cm}^{-1}$ . This shift took place as more of the amine was neutralized that also resulted in a decrease in the absorbance magnitude as seen in Figure 0-1. In Figure 0-2, a decrease in the peak around  $6400\text{ cm}^{-1}$  was observed with higher degrees of neutralization for the second overtone region. This could also be accounted by the fact that less of the un-neutralized amine was present in the solution. Lastly, the most noticeable change of absorbance was observed at the 3<sup>rd</sup> overtone region. As seen in Figure 0-3, 0% DoN had the highest peaks at  $8700\text{ cm}^{-1}$ , whereas higher degrees of neutralizations had lower ones.

A calibration model using these three overtone regions was developed to assess how useful these overtones could be in determining the degree of neutralization of the solution. The following two figures, 0-4 and 0-5, represent the calibration model developed along with its residual error plot.

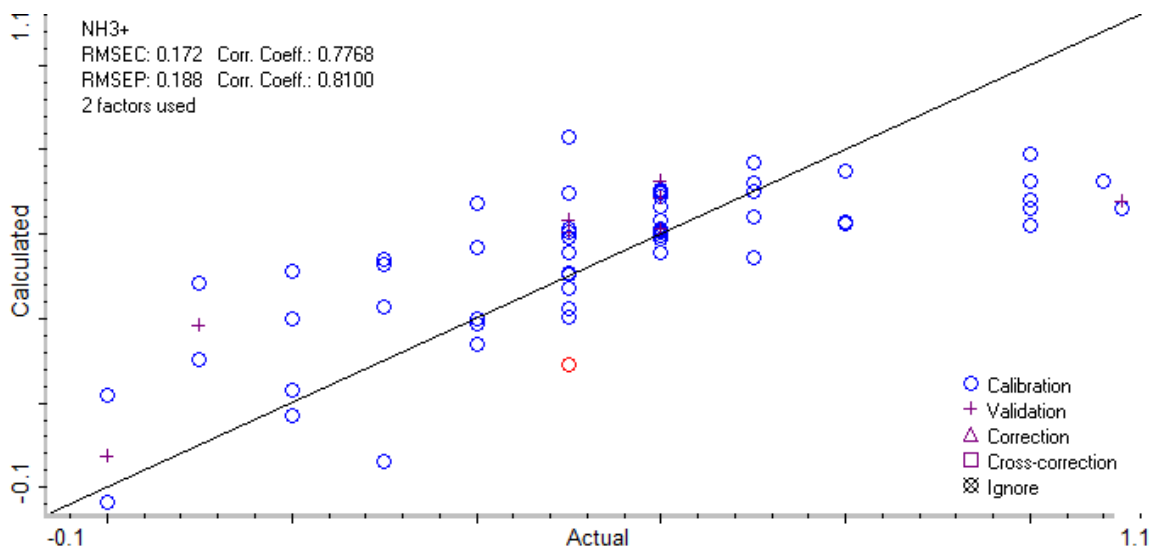


Figure 0-4: Calibration model using the three amine overtone regions after smoothing filters were applied.



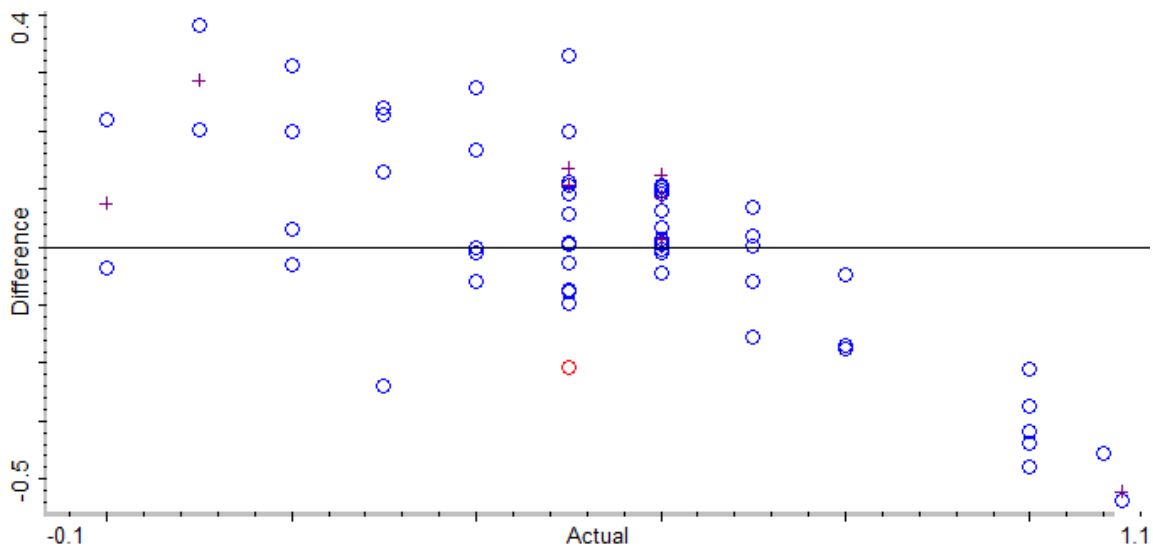


Figure 0-5: Residual error plot using the three overtone regions of amine after smoothing filters were applied.

The calibration model was unable to predict the degree of neutralization within the required minimum margin of error,  $\pm 6\%$  DoN, in comparison to  $\pm 45\%$  DoN. Although there were trends observed as the degree of neutralization changed, these trends were not consistent throughout the absorbance spectra. Minimal changes in the water flowrate introduced a lot of noise into the spectra that made it difficult to infer and relate between the absorbance magnitude and its corresponding neutralization degree. In comparison, the chosen region of  $4400\text{-}4250\text{ cm}^{-1}$  was not affected by changes to the water flowrate since water was not absorbed within that region. That region was only affected by the amount of amine that was neutralized. Over additions of hydrochloric acid did not impact the spectra which made it more appealing to use as the basis for chapter six rather than the three amine overtones.